REEF RESTORATION & ADAPTATION PROGRAM

Applied science material for coral aquaculture (3.1.3-4Q4)

09 September 2024

Elsa Antunes, Matthew Drane, Georgia Astbury, Florita Flores, Jenny Fong, Andrew Negri, Andrea Severati, Muhammad Abdul Wahab

Applied science material for coral aquaculture (3.1.3-4Q4)

Enquiries should be addressed to:

Elsa Antunes – elsa.antunes1@jcu.edu.au

Muhammad Abdul Wahab - M.AbdulWahab@aims.gov.au

Andrea Severati - A.Severati@aims.gov.au

[*Cover Page: Image Caption, Credit*]

[Image 4: Coral Reef, Credit: Gary Cranitch, Queensland Museum]

This report should be cited as

Elsa Antunes, Matthew Drane, Georgia Astbury, Florita Flores, Jenny Fong, Andrew Negri, Andrea Severati, Muhammad Abdul Wahab. (09/09/2024) Reef Restoration and Adaptation Program – Applied science material for coral aquaculture (3.1.3-4Q4), pp. 38.

Acknowledgement

This work was undertaken for the Reef Restoration and Adaptation Program (RRAP). Funded by the partnership between the Australian Governments Reef Trust and the Great Barrier Reef Foundation, partners include: the Australian Institute of Marine Science, CSIRO, the Great Barrier Reef Foundation, Southern Cross University, the University of Queensland, Queensland University of Technology and James Cook University.

The RRAP partners acknowledge Aboriginal and Torres Strait Islander Peoples as the first marine scientists and carers of Country. We acknowledge the Traditional Owners of the places where RRAP works, both on land and in sea Country. We pay our respects to elders; past, present, and future; and their continuing culture, knowledge, beliefs, and spiritual connections to land and sea Country.

Table of Contents

1 Materials for asexual propagation

The main objective of the asexual propagation experiment was to investigate the impact of materials chemistry (chemical composition) and physical properties (porosity, toughness, etc.) on corals survival rate and growth. In this experiment six different materials were tested: (1) alumina, (2) concrete, (3) glass, (4) polyvinyl chloride, (5) aragonite and (6) composite of biopolymer and $CaCO_3$. The surface texture and porosity of some materials were manipulated, thus in total we tested 13 combinations of materials with different chemical composition and/or physical properties. Fragments from *Acropora millepora*, *Platygyra daedalea* and *Porites lutea* were attached to each substrate material tile to assess their survival and growth in aquaria.

1.1 Materials Preparation

Figure 1 schematically presents eleven different tile materials and surface configurations that were tested, with a naming convention to refer to the materials throughout the report. Glass and PVC were also tested but without any surface modification.

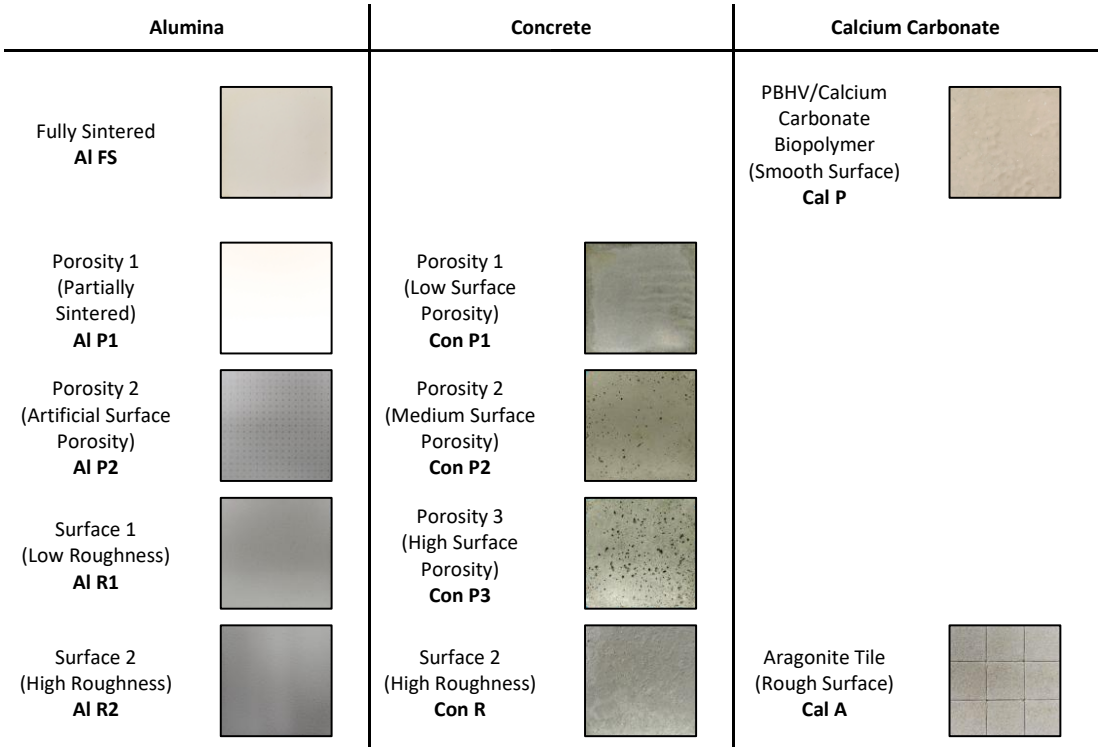

Figure 1: Experimental design for comparison of material composition and surface structure.

The **concrete samples** were prepared following the standard AS 2350.12 – 2006 section 6 and 7 [1]. Adaptation of the standard mold size to a 90 x 90 x 10 mm PVC mold was made to achieve the desired dimensions to fit in the experimental tanks. The duration of time on the vibration table was modified to achieve variation in porosity. The tiles were leveled with a straight edge and placed in a controlled humidity and temperature chamber to cure. Chamber was set at a humidity of 90% and a temperature of 25°C. They were retained in the mold for 24 hrs before being removed and left in the controlled humidity and temperature climate for another 6 days at the same conditions. Figure 2 shows the variation in tile surfaces prepared. A vibration duration of 4 minutes was used to produce 18 tiles. The molded surface of nine tiles called 'Concrete Porosity 1', and the top screeded surface of the remaining nine tiles being categorized as 'Concrete Rough'. 'Concrete Porosity 2' was achieved for nine tiles by reducing the vibration time to 2 mins. 'Concrete Porosity 3' were produced from a vibration time of 1 min. The average surface porosity, assessed by photo imagery of the tiles is summarized in Table 1.

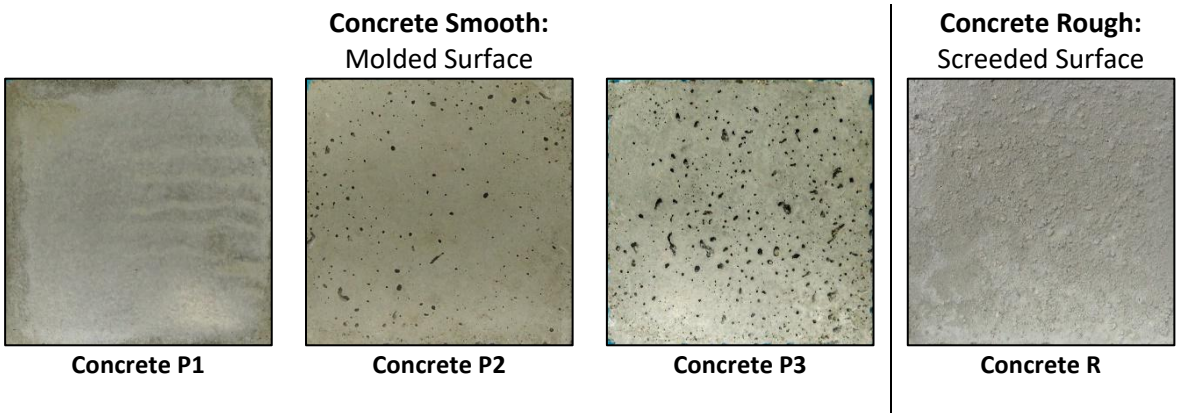

Figure 2: Representative Tiles for Concrete Surfaces.

Table 1: Concrete Substrate Average Surface Porosity.

Concrete Sample	Surface Porosity (%)
P1	0.58
P2	2.75
P3	5.99

Fully sintered **95% pure alumina** tiles were sourced from Gongtao Ceramics, Shanghai, and used with no further surface modification. **Partially sintered alumina** tiles (Alphoxit 100) were sourced from Alpha Ceramics GmbH, Germany. Nine tiles were used with no surface modification and categorized as 'Alumina Porosity 1'. An artificially porous surface 'Alumina Porosity 2' was achieved by drilling holes 1.5 x 1.5 mm (D x H) at spacing of 5 mm using a tungsten-carbide tool. These two tile preparations are presented in Figure 3. Two different surface roughness profiles were achieved through sand blasting at 100 psi with garnet grade 50/80, sourced from Burwell Technologies, Townsville. A lower roughness surface named 'Alumina roughness 1' was achieved by evenly passing the sandblasting gun across the surface at approximately 40 cm from the surface. A higher level of roughness was achieved by decreasing the distance of the sandblasting gun to approximately 30 cm and increasing the duration of time taken for each pass of the sandblasting gun.

Figure 3: Partially Sintered Alumina Tiles with artificially modified surface porosity.

Aragonite tiles were purchased from Aquasonic as Coral Frag Tiles Aragonite, OW100CFT. To produce tiles of comparable dimensions the aragonite tiles were joined with West Systems Epoxy Resin 105 and hardener 206,

in addition to West Systems 403 microfiber blend adhesive filler. It was ensured that the epoxy was not being placed onto the growing surface available to the corals. Tiles were clamped and held at 25°C for 24 hrs to cure.

A **PBHV and calcium carbonate composite (Biopolymer)** was produced at the Royal Melbourne Institute of Technology (RMIT). The composition of the composite was reported at a ratio of 60wt%:40wt%, PBHV:$CaCO_3$.

Standard textured **glass** (white acid etched) and **polyvinylchloride** (PVC; smooth) tiles were sourced from local suppliers in Townsville, Australia. These two materials were used as a control.

1.2 Materials Characterization

Material characterization was performed to determine the key features of each material including the surface topography and structure, porosity, and chemical composition. The results of this characterization allow for an overview of the parameters which have the most influence on coral growth and survival rate for asexually reproduced corals.

1.2.1 Surface Roughness

The surface roughness of the different materials was characterized with laser scanning microscopy (LEXT OLS4100, Olympus Corporation, Japan Instrument). Five random areas of 2.583 x 2.574 mm were scanned of each material sample to obtain a 3D surface profile image. Figure 4 shows the areal parameters of arithmetic mean height, S_a, Equation 1 and maximum height, S_z, Equation 2, which were measured and recorded through LSM. Additionally, a representative 2D horizontal and vertical profile were also plotted along one randomly chosen x-axis and y-axis location for each sample.

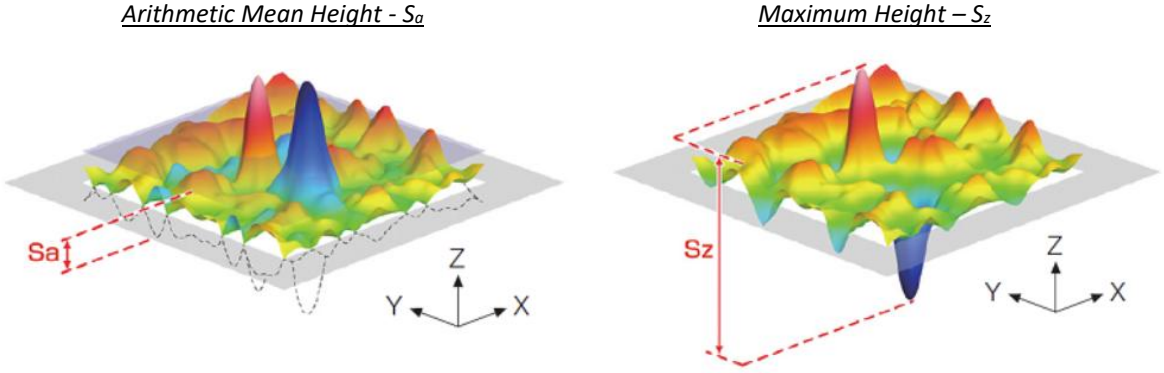

Figure 4: Visual representation of arithmetic mean height and maximum height parameters.

$$S_a = \frac{1}{A}\iint_A |z(x,y)|\,dxdy \quad (1)$$

Where A is the area being evaluated.

$$S_z = S_p + S_v \quad (2)$$

Where S_p is the maximum peak height and S_v is the maximum pit depth.

Surface roughness measurements through LSM provide an understanding of the topographical structure of the material surface at a microscopic scale. The surface roughness is an important parameter to measure for the various materials as this is the surface which the coral is growing on top of. Determination of the mean roughness and maximum height of the roughness surface enables identification of roughness best suited to enable coral growth, whether asexual propagation of coral is better suited to rough or smooth surfaces. The maximum height (S_z) provides an understanding of the sum of the maximum peak and maximum pit height. It is noted however that the S_z parameter is based on peak values and hence can be influenced by factors such

as scratches and measurement noise. The arithmetic mean (S_a) provides the average height of the sample profile for the area evaluated [2]. This parameter is less affected by scratches and measurement noise and can be used as a more reliable comparison between samples.

The mean roughness (S_a) results show similar trends to that of the maximum height (S_z) values with aragonite surface being the roughest surface while the alumina P1 is the smoothest. Comparison of the alumina samples trialled shows the surface preparation techniques and different sintering conditions achieved a range of surface profiles. Alumina smooth has the lowest variation in surface profile with a mean roughness of 1.25 µm. This measurement is representative of Al P1 and the horizontal surface Al P2 as this surface was modified from P1 only through the drilling of holes 1.5 mm x 1.5 mm (D x H). This surface modification is of a larger scale surface to the roughness measurement than possible with LSM. The fully sintered alumina sample has a higher roughness than expected with a reported mean roughness of 5.54 µm. The two-dimensional profile presented in Figure 7 (a) shows high variation in the profile with sharp peaks and valleys. The partially sintered alumina samples prepared through sand blasting, Al R1 and Al R2 show similarity in roughness height and mean roughness values where the peak to valley height is 5% higher for Al R2. This similarity is expected due to the same sandblasting grain size being used for both samples.

Comparison of the concrete surface roughness profiles indicates clear differences in magnitude of the surfaces depending on the preparation technique. Two concrete surfaces were compared, the smooth moulded surface and rough screeded surface. The smooth surface is representative of Con P1, P2, and P3 as the open porosity is of dimensions higher than the magnification of the LSM analysis. The smooth concrete surface is found to have a mean height of 2.38 µm compared to a mean height of 8.47 µm for the rough concrete surface. Comparison of the 2D and 3D profiles of the two concrete surfaces, Figure 7 (f), and (g), also clearly shows this variation in surface microtopography. With high irregularity and waviness observed for the rough surface while the profile for the smooth concrete is more constantly maintained at the same level with only small variations in height.

Aragonite is the roughest substrate material tested. It is found to have both the largest maximum height of 629 µm and mean arithmetic height of 10.2 µm. The three-dimensional profile Figure 7 (e) shows the material has a high degree of waviness, with the surface being highly irregular in both the x and y planes.

The PBHV:CaCO3 biopolymer shows one of the lowest roughness profiles. The surface profile shows low degree of waviness indicating that the material is relatively smooth across entire surface.

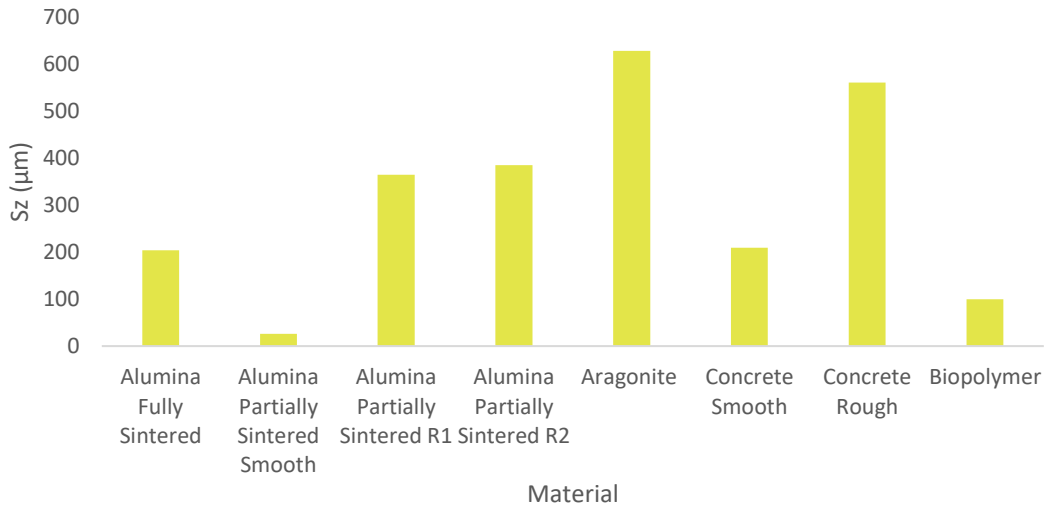

Figure 5: Maximum height variation of settlement substrate materials.

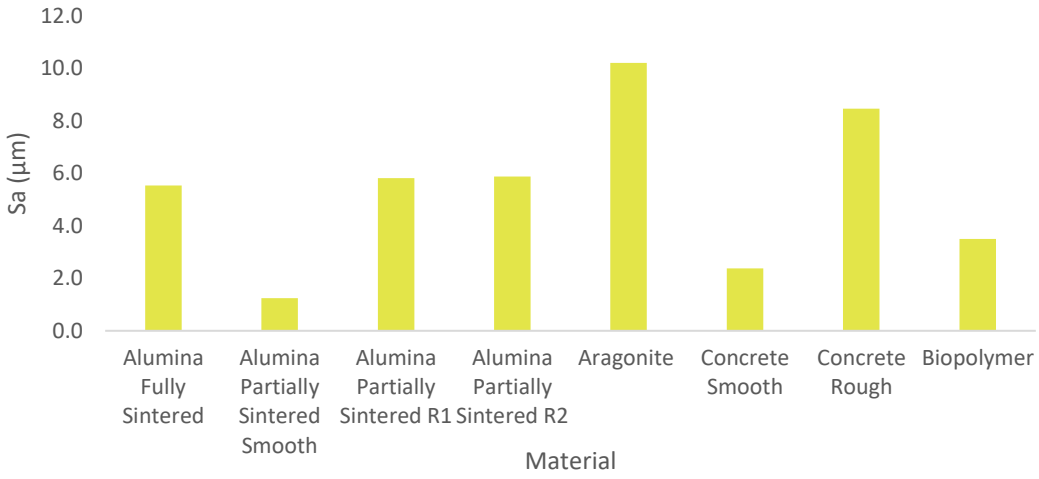

Figure 6: Arithmetic Mean Height of Settlement Substrate Materials.

To compare the relative performance of different surfaces with similar roughness, a scale was developed based on the results presented for mean roughness in Figure 6. This enables the categorisation of the materials into low, medium and high roughness for quantification of coral growth based on surface characteristics, and to assess the varying level of influence which both the material type and surface topography have on coral growth. Table 2 summarises the mean surface roughness categories and the corresponding materials.

Table 2: Surface Roughness Categories.

Roughness Level	Mean Surface Roughness Range	Materials
Low	0 – 4 µm	Al P1 Con P1 Con P2 Con P3 Biopolymer
Medium	4 – 8 µm	Al FS Al R1 Al R2
High	< 8 µm	Con R Aragonite

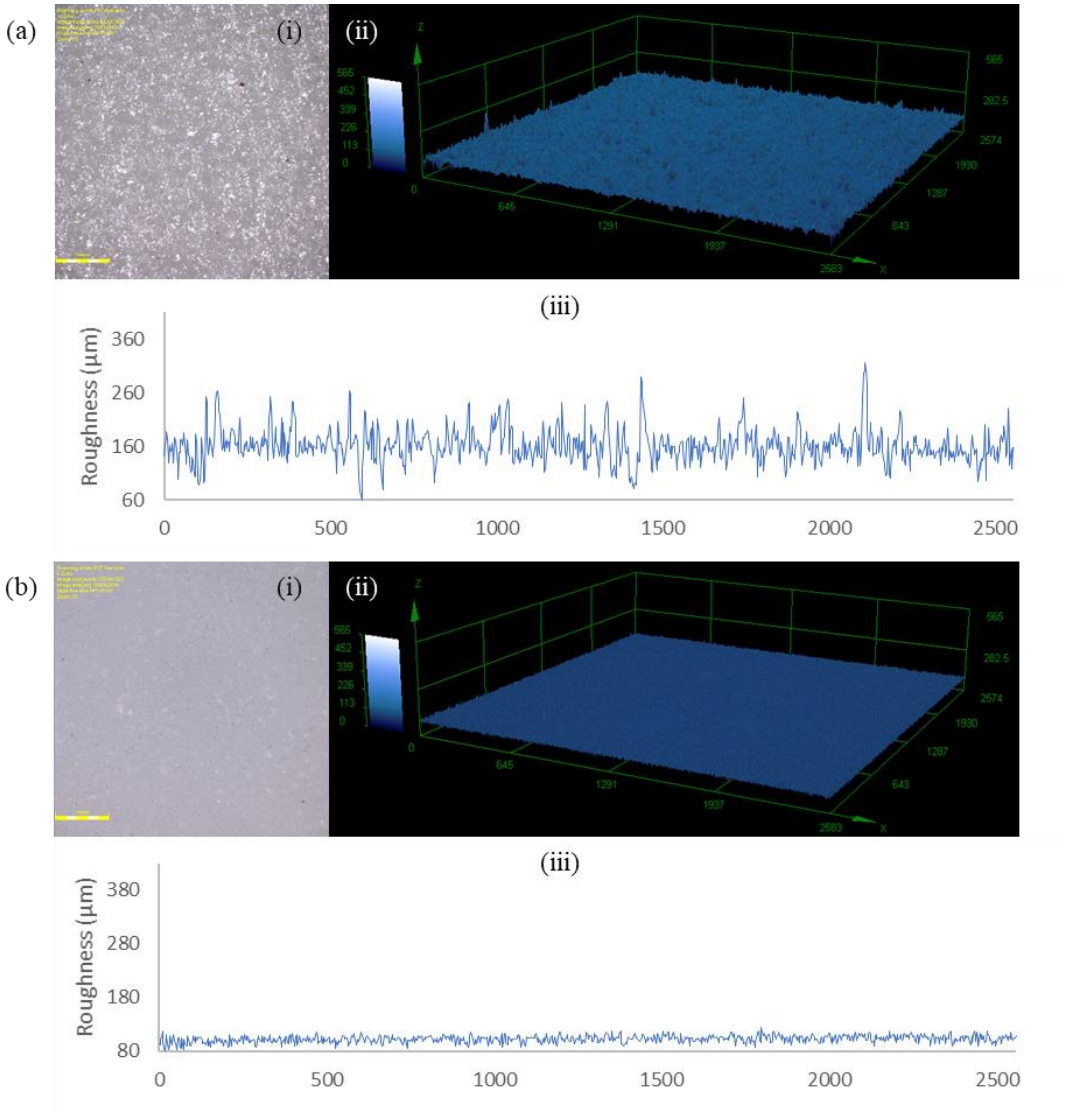
(a)
(i)
(ii)
(iii)
Roughness (µm)
360
260
160
60
0
500
1000
1500
2000
2500
(b)
(i)
(ii)
(iii)
Roughness (µm)
380
280
180
80
0
500
1000
1500
2000
2500

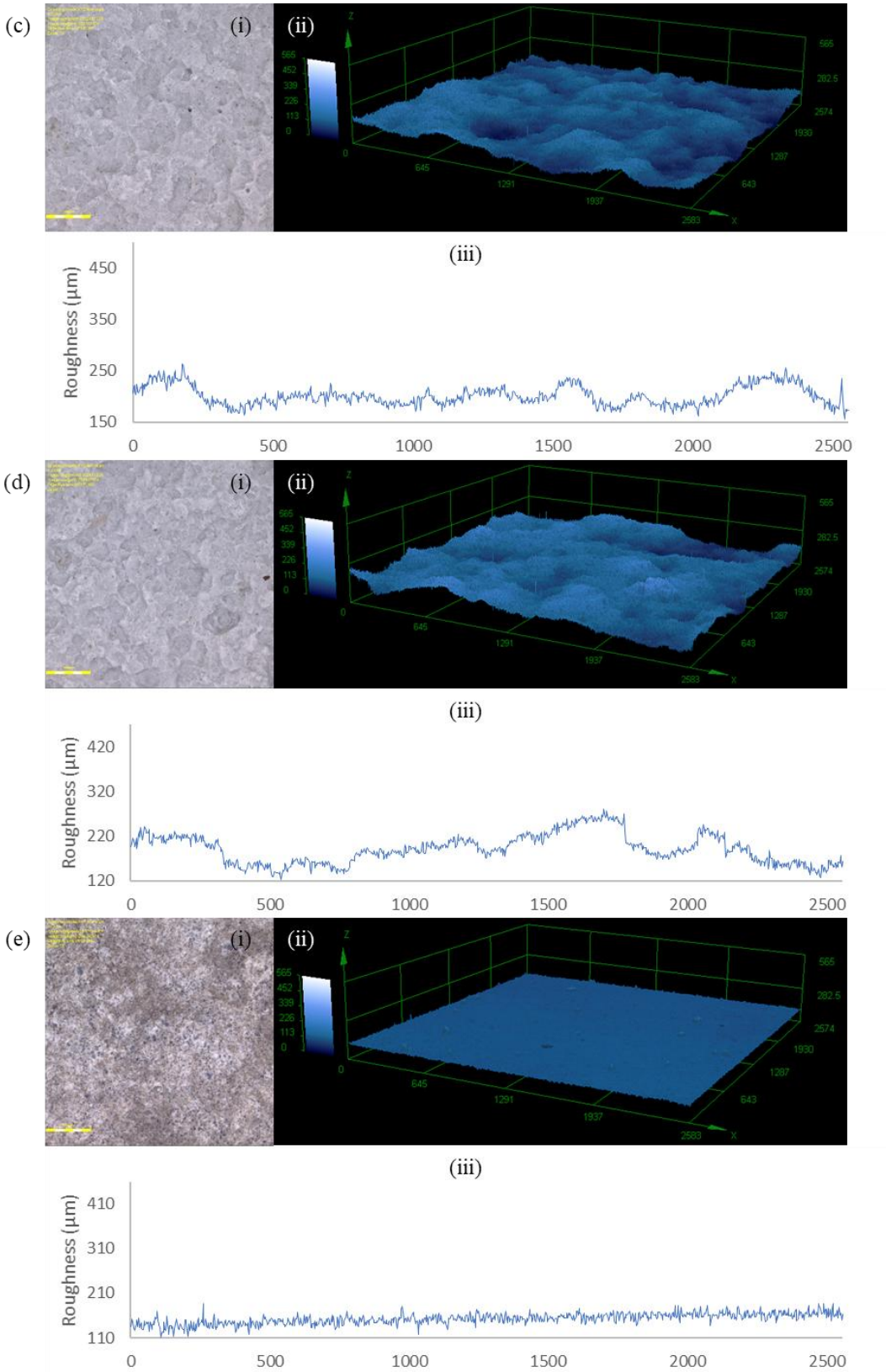
(c)
(i)
(ii)
(iii)
Roughness (µm)
450
350
250
150
0
500
1000
1500
2000
2500
(d)
(i)
(ii)
(iii)
Roughness (µm)
420
320
220
120
0
500
1000
1500
2000
2500
(e)
(i)
(ii)
(iii)
Roughness (µm)
410
310
210
110
0
500
1000
1500
2000
2500

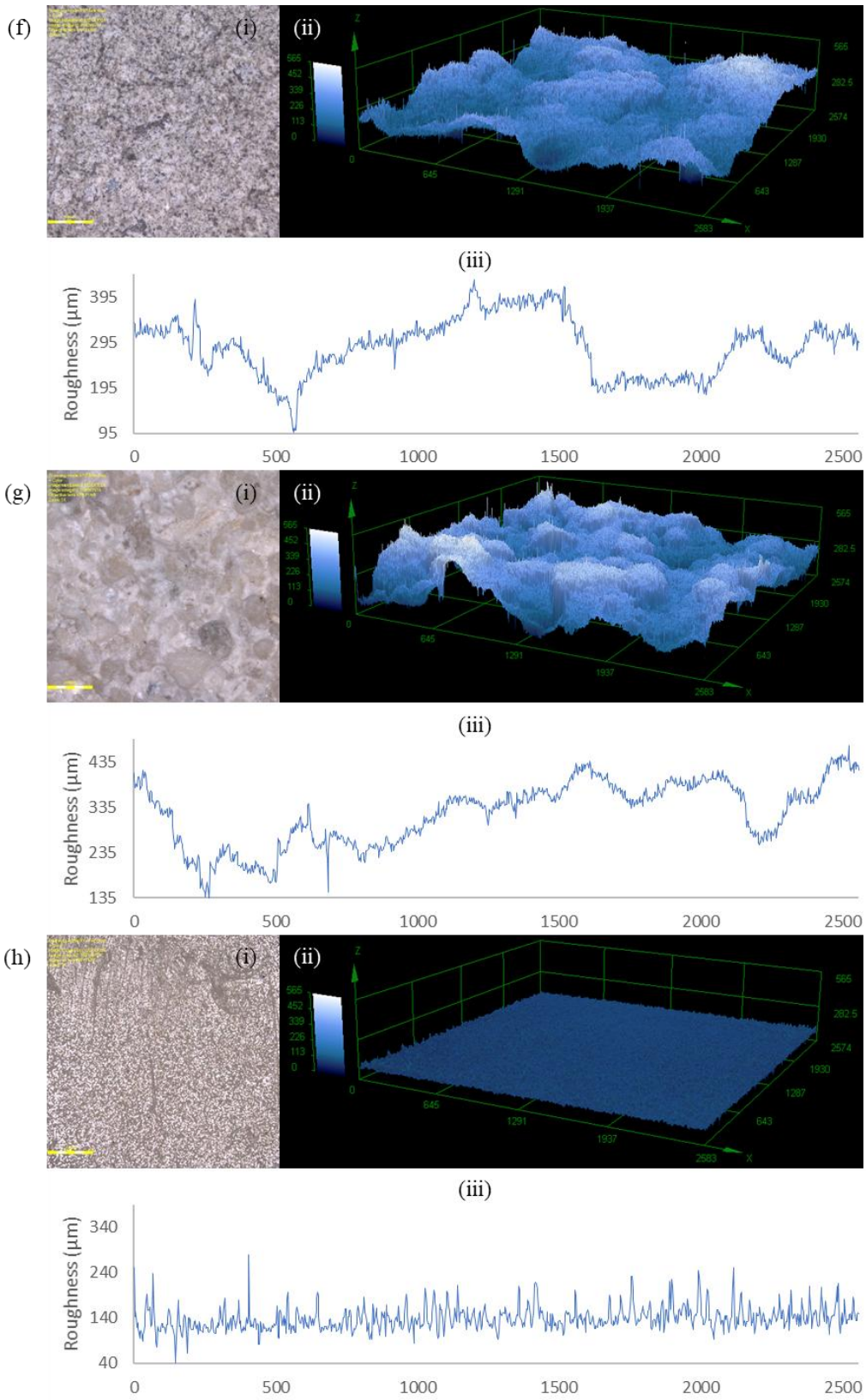

Figure 7: LSM (i) Surface Image, (ii) 3D Roughness Profile; (iii) 2D Roughness Profile along x-axis for: (a) Alumina Fully Sintered; (b) Alumina Partially Sintered Smooth; (c) Alumina Partially Sintered Roughness 1; (d) Alumina Partially Roughness 2; (e) Aragonite; (f) Concrete Smooth; (g) Concrete Rough; (h) PBHV Biopolymer.

1.2.2 Scanning Electron Microscope (SEM)

Scanning Electron Microscope (SEM) is an analytical technique which produces high resolution 2D images of a sample surface at high levels of magnification. A beam of high-energy electrons is directed at the surface, the interaction of the electrons with the sample produces secondary electrons and backscattered electrons, which are detected to produce an image. SEM (Jeol JSM5410LV) was used to determine the microscopic surface morphology of representative samples of the settlement substrates. The samples were placed on carbon adhesive tape and coated with platinum to ensure the samples were electrically conductive and accurate results could be obtained. Three random locations were selected for each sample and imaged at three different magnifications of 5 µm, 20 µm, and 100 µm.

Coupled with Energy-dispersive X-ray spectroscopy (EDS), SEM-EDS enables the qualitative determination of the sample chemical composition. An SEM-EDS Detector (Instrument: Jeol JXA8200) was utilized to analyze the chemical composition of each material. This was performed at a magnification x200.

SEM images enable identification of the grain size and surface pore structure of the material. The coral grows across and attaches to this surface. In combination with the surface roughness results obtained through LSM, SEM images can provide further characterisation to the types of surfaces which assist coral attachment and growth for asexual propagation.

SEM images at three different magnifications of 500x, 2000x, and 10000x were used to achieve an understanding of the surface topography and structure for the eleven different material and tile surfaces tested. Due to the SEM images analysing microscale topographical variations, Alumina P1 is representative of alumina P1 and P2 which vary in macro scale topography only. Additionally, the smooth concrete surface is representative of concrete P1, P2, and P3.

SEM images in Figure 8 (a), (b), (c), and (d) show comparison of the four alumina samples Al FS, Alumina P1 representative of P1 and P2 surfaces, Alumina R1 and R2. Fully sintered alumina (Al FS) shows low porosity as expected, but the surface is uneven with jagged angular microstructure. The surface is much more irregular than that of Al P1. This supports the results obtained from the surface roughness LSM measurements. The partially sintered alumina material Figure 8 (b), (c), and (d) show similarity in grain structure across the samples. This is a homogenous distribution of fine spherical grains since the material is partially sintered. This is because Al P1, P2, R1 and R2 are all manufactured from the same base material. The Al R1 and Al R2 materials vary from Al P1 in the surface topography, while the grain structure is the same, there is higher irregularity with larger scale peaks and valleys. As identified in the LSM analysis, the variation between the two rough alumina samples (R1 and R2) is not large, however the irregularity of the surface is more prevalent in the R2 sample with a higher degree of irregularity.

Comparison of the smooth and rough concrete surfaces, Figure 8 (f and g), show clear topographic and grain size variations between the two preparation techniques. The smooth surface Figure 8 (f) has a smaller grain size in contrast to the rough surface Figure 8 (g). The rough surface is highly irregular due to the large sand grains present at the surface. The preparation of the smooth tile surface by moulding means that the fine grains settle across the smooth mould surface. In contrast preparation of the rough tiles through screeding of the surface generates a rough surface dominated by larger sand grains.

The aragonite material (Figure 8 e) shows high variation in the surface microtopography. The surface shows a high degree of large open pores. The surface is also highly irregular which supports the results obtained through LSM.

The PHVB:CaCO3 Biopolymer (Figure 8 h) has a very smooth, homogenous surface topography. No evidence of calcium carbonate particles is present on the surface of the polymer material. Limitations in the magnification for SEM were reached due to the low melting point of the polymer material.

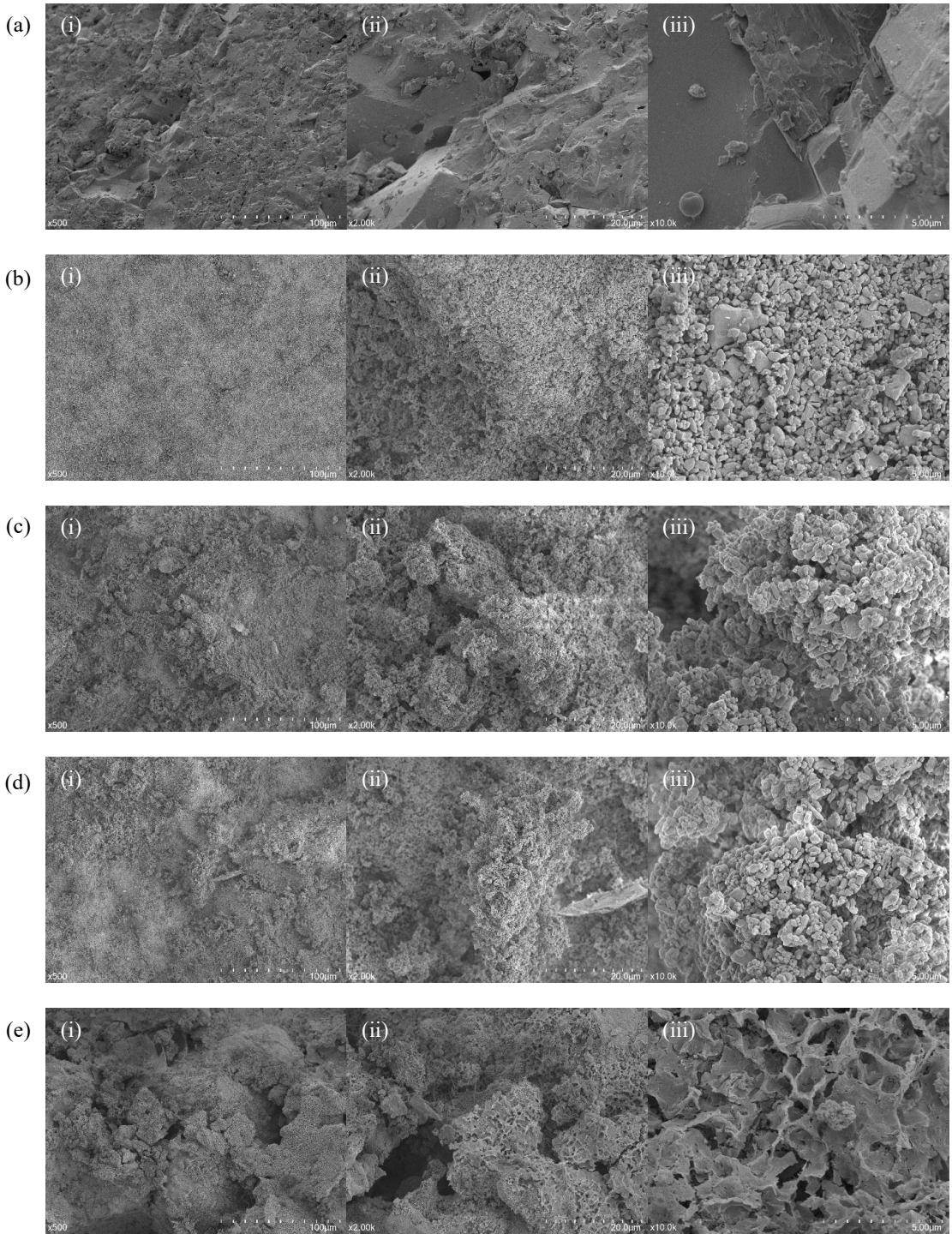
(a)
(i)
(ii)
(iii)
(b)
(i)
(ii)
(iii)
(c)
(i)
(ii)
(iii)
(d)
(i)
(ii)
(iii)
(e)
(i)
(ii)
(iii)

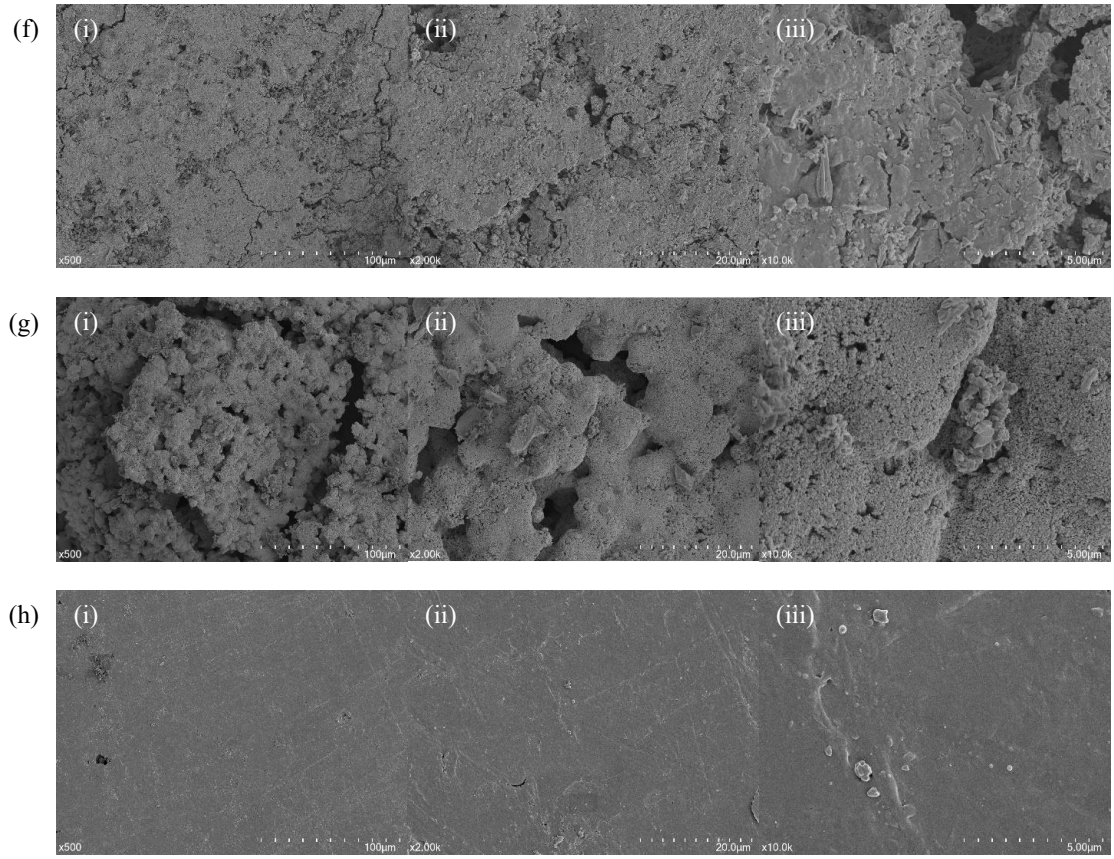

Figure 8: SEM images at (i) 100µm, (ii) 20µm and (iii) 5µm scale of substrate samples: (a) Alumina Fully Dense; (b) Alumina Porosity 1; (c) Alumina Roughness 1; (d) Alumina Roughness 2; (e) Aragonite; (f) Concrete Smooth Surface; (g) Concrete Rough Surface; (h) PHVB:CaCO3 Biopolymer.

SEM-EDS was used to determine the chemical composition of the materials. Identification of the material composition at the surface of attachment enables further identification as to the importance of the chemical composition of the substrate opposed to the physical surface topography of the material. The results obtained from SEM-EDS are present for each substrate material in Figure 9. Oxygen was present in high levels between 47 and 71 wt% in all samples.

Purity of the alumina samples are high, with 52 wt% aluminum present in both samples. Small levels of impurities of silicon are present in both partially sintered and fully sintered alumina samples. Additionally, trace amounts of calcium are present in both with the fully sintered alumina reporting 0.1 wt% and 0.06 wt%. These values are very low and may be due to sample contamination.

The concrete samples are found to have similar elements present on either surface. It is noted that the aragonite sample also contains these same elements in corresponding levels. Calcium is the element in highest concentration for all three material surfaces. The SEM-EDS analysis reporting 24.02 wt% for the rough side of concrete which is lower than the 26.80 wt% reported for the smooth side. The aragonite reports a value of 25.65 wt%. These values are much higher in weight percentage than the reported value of 2.51 wt% for the calcium carbonate doped biopolymer. Carbon is an element also prevalent in the concrete and aragonite samples at a wt% between 11.99 and 15.51 wt% for the three materials which exhibit similar chemical makeup. While carbon is not present in the alumina samples, slightly higher values than the concrete based materials are reported for the polymer at 26.26 wt%. Silicon is noted to be of a higher concentration in the two concrete surfaces and aragonite. The highest concentration is present on the smooth surface of the concrete at 4.76 wt%, the aragonite and rough concrete surfaces are of similar magnitude of 3.06 wt% and 2.36 wt%, respectively. Trace metals present in the three materials include potassium, iron, along with sulfur are noted to be only present in these samples of concrete and aragonite. Analysis of the chemical composition of these samples shows that the concrete and aragonite samples have very comparable chemical makeup.

The chemical composition of the biopolymer indicates that on the surface of the material it has 2.5 wt% calcium carbonate. This equates to a 6.3 wt% calcium carbonate in the polymer. Although EDS is a qualitative analysis of the chemical composition and provides an overview of the elements present, this value is considerably lower than the expected 40 wt% calcium carbonate composition of the material. The overall purity of the sample is relatively high with only trace levels of magnesium, aluminum and silicon.

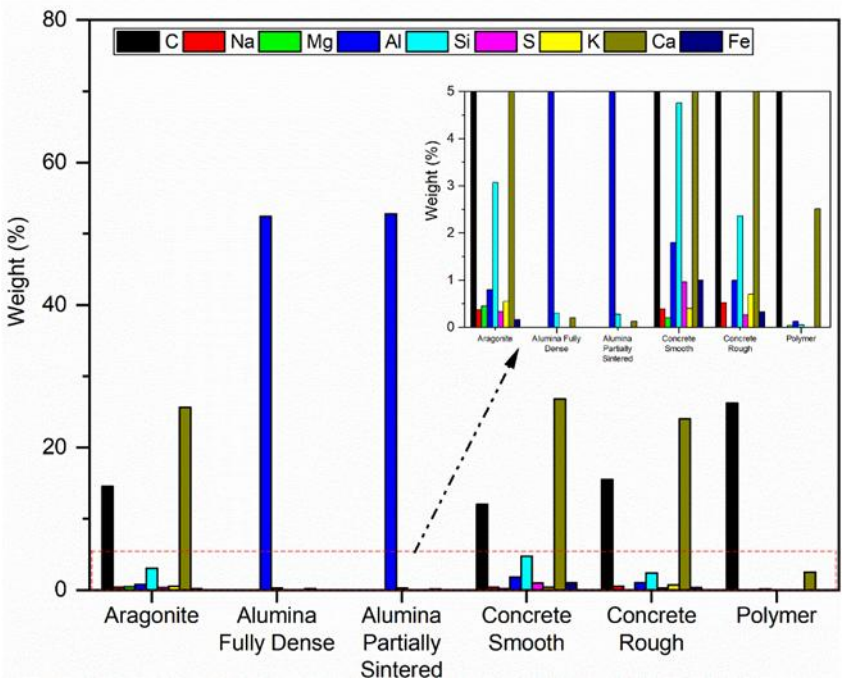

Figure 9: Elemental composition of each material by weight percent. Elemental symbols: C – carbon, Na – sodium, Mg – magnesium, Al – aluminium, Si – silicon, S – sulphur, K – potassium, Ca – calcium and Fe – iron.

1.2.3 Porosity Measurements

The bulk density, apparent solid density and apparent porosity of the samples was determined according to the method outlined in International Standard ISO 18754 – 'Fine ceramics (advanced ceramics, advanced technical ceramics) – Determination of density and apparent porosity' [3].

The dry mass, m_1, was determined through weighing the dry sample. Samples were then fully submerged in a beaker of water. The beaker was covered in aluminium foil and placed in an oven at 100°C for 3 hours. Samples were removed from the oven and the individually transferred to a beaker with water at 23°C ambient temperature for 15 mins. The soaked mass of the sample was obtained by taking the sample from the water, removing any excess water with paper towel and placing on the balance. This mass was recorded as soaked mass m_3. Apparent mass, m_2 was obtained by placing the sample in a basket suspended in water, the suspended mass of the sample was measured on the balance. Water temperature was measured at 23°C which correlates to a density of water of 997.5 kg/m^3 in the standard Table 1. The following calculations were used to determine the bulk density, apparent solid density and apparent porosity of the materials tested:

Bulk density:

$$\rho_b = \frac{m_1}{m_3 - m_2}\rho_w \qquad (3)$$

Apparent solid density:

$$\rho_a = \frac{m_1}{m_1 - m_2}\rho_w \quad (4)$$

Apparent porosity:

$$\pi_a = \frac{m_3 - m_1}{m_3 - m_2} \times 100 \quad (5)$$

The density of the substrate materials and apparent porosity of the samples were measured to determine if the porosity throughout the material has an influence on coral growth. Apparent solid density is a measure of the ratio of dry material mass to combined volume of solid and closed pore volume. The bulk density is the ratio of dry mass to total volume including open pores, closed pores and the volume of solid material in the sample [3]. Apparent porosity is the ratio of total open pore volume to the material bulk volume, the addition of solid, open, and closed pore volume.

Figure 10 compares the apparent solid density and bulk density of the substrate material samples. The fully and partially sintered alumina samples have the highest apparent solid density. This is a measure of density excluding the air voids. Similarity in values between the two alumina samples is due to the similar chemical composition. The porosity between the sintered and partially sintered materials varies as expected. The sintered alumina has the highest bulk density, and correspondingly a low apparent porosity. While the apparent porosity of the partially sintered sample is high at approximately 37%. The partially sintered material as seen in the SEM images has granular particles which allow air voids throughout the material and hence the high porosity. Artificial surface porosity was tested for the substrate Al P2, this is calculated to be an added surface porosity of 6.3% based on the 1.5 mm diameter holes drilled at regular spacings of 5 mm apart.

The concrete surface porosity varies between the samples. Figure 11 indicates the smooth concrete has the lowest surface porosity 0.58%, the highest surface porosity being P3 with a surface porosity of 5.99%. Although the macro-open pores on the surface of the material vary between the samples, the internal porosity does not vary significantly. Notably, the bulk density, apparent solid density and apparent porosity values determined for the aragonite sample is also comparable to the concrete materials. This further indicates comparable properties between the concrete and aragonite substrate materials.

The polymer is the material with the lowest density of the substrates tested. The apparent density and bulk density are determined to be similar due to the low apparent porosity of the sample as seen in Figure 10. The porosity measured for the polymer is comparable to the low porosity of the fully sintered alumina tiles.

For analysis of the performance of materials with different porosity, the categories of low, medium, and high porosity are used to class the materials and enable comparison, as summarized in Table 3. The biopolymer and fully sintered alumina tiles are categorized into low porosity with less than 10% apparent porosity. All concrete samples and the aragonite are determined to have similar apparent porosity in the range of 10 to 20% and categorized as medium porosity. The partially sintered alumina tiles are shown to have high porosity with apparent porosity greater than 20%.

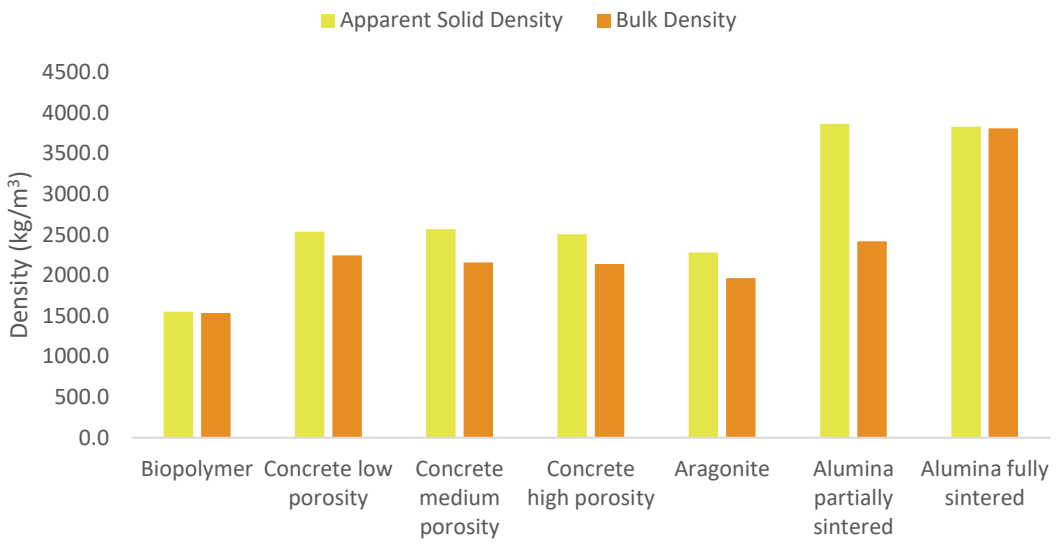

Figure 10: Apparent solid and bulk densities for each material.

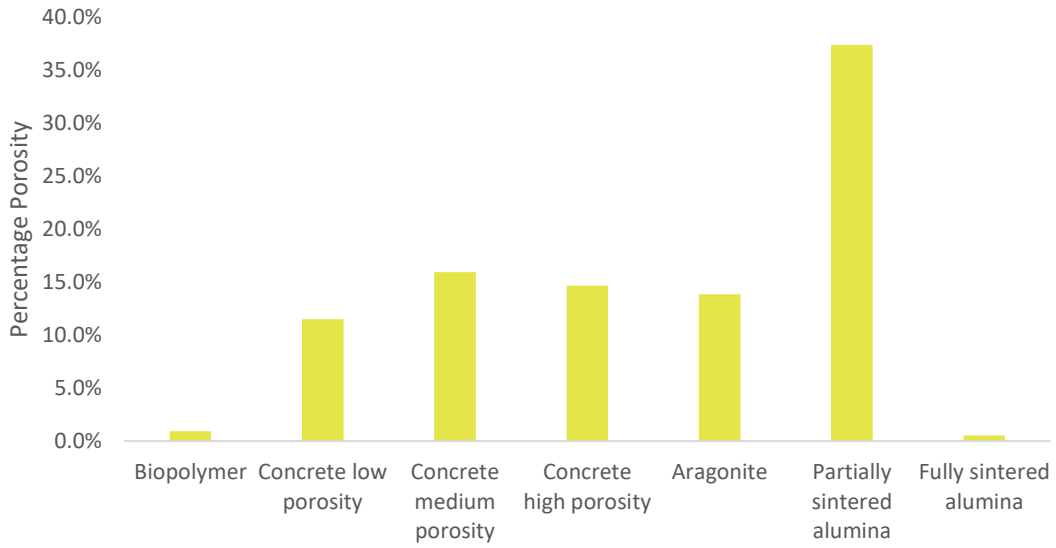

Figure 11: Apparent Porosity for each material.

Table 3: Porosity Categories.

Porosity Level	Apparent Porosity Range	Materials
Low	0-10%	Pol Al FS
Medium	10-20%	Con P1 Con P2 Con P3 Con R1 Aragonite
High	20%+	Al P1 Al P2 Al R1 Al R2

1.2.4 Coral Fragging and Propagation

For this experiment, six colonies of the of the corymbose *Acropora millepora*, massive *Porites lutea* and sub-massive *Platygyra daedalea* were collected from depths of 1–6 m from reefal habitats at Davies Reef (18°49'12.2"S 147°38'39.4"E) and Falcon Reef (18°76'64.8"S 146°53’55"E), central Great Barrier Reef (GBR), between 29th April to 10th May 2021 (GBRMPA Permit G21/45348.1).

The coral fragments were cut using a combination of diamond blade circular saw and bandsaw to achieve approximate dimensions of 14 x 14 x (1-6) mm (L x W x H). Only the outer growth of the coral colony surface was used for the experiment. The newly cut frags were immediately attached to the substrate surface using approximately 3 drops of super glue (Gorilla Super Glue Precise Gel an Ethyl Cyanoacrylate Adhesive) and replaced into filtered saltwater tanks. Nine frags are placed per tile at spacings of 16 mm apart and 8 mm from the sides as in Figure 12. A total of three replicate tiles of the same genotype for each material were prepared. The tiles were randomised into three separate tanks, placed in racks at an angle of 65°.

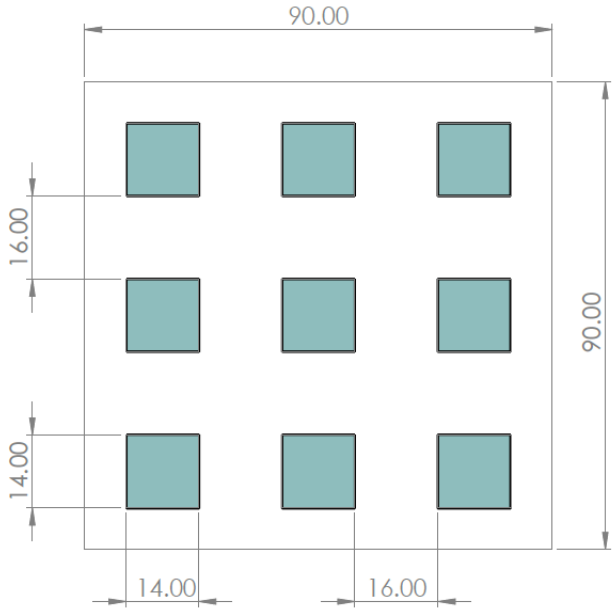

Figure 12: Coral Frag Arrangement on Tile.

The experiment was carried out in the AIMS National SeaSimulator. Lights were set at max par 120 µmol with daily light/lunar cycles that match Townsville. Daily water temperature profiles were set to match Davies Reef, the location the coral colonies were sourced from. The experiment was carried out in three tanks with incoming filtered sea water to 1 micron and salinity corrected to approximately 35 ppt. Water flow is generated in the tanks using two Maxspect gyres, with fresh salt water in the tanks is recirculated with three full turnovers per day.

Overall, all the materials were found to be suitable settlement substrates for coral growth. Each material was shown to enable growth of the coral on the surface throughout the experiment, with all substrate materials maintaining mechanical stability in the marine conditions. Representative images at the initial time point of testing and at the completion of testing at nine weeks is presented for each of the 11 materials in Figure 13. General observations of the coral frags show that coral new growth extends out from the perimeter of the coral frag along the surface of the substrate material. The growth rate of the coral is the increase in the two-dimensional surface area covered by coral at each data collection time point.

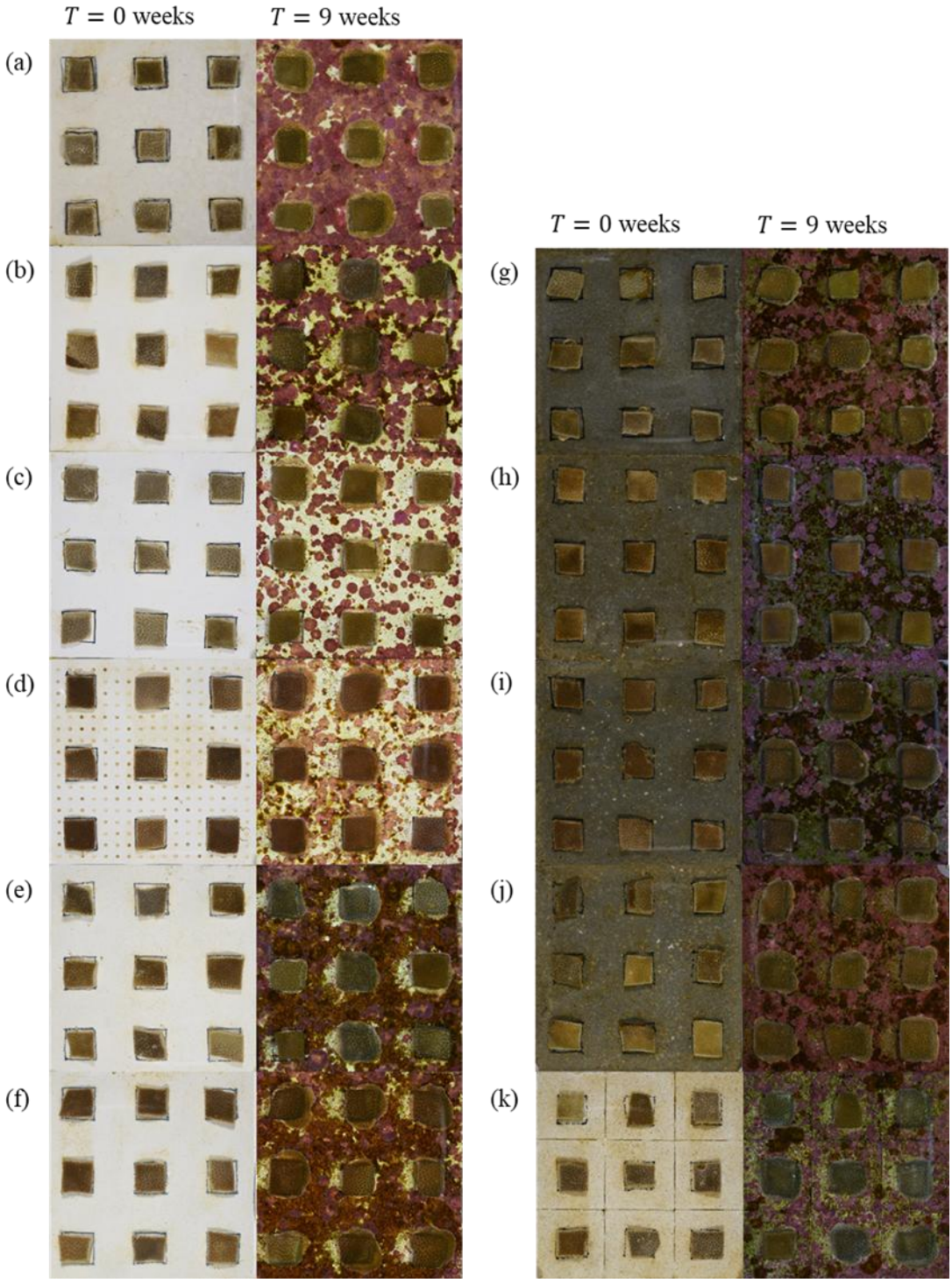

Figure 13: Nine week growth of coral and fouling organisms on eleven substrate materials: (a) PBHV:$CaCO_3$ Biopolymer; (b) Alumina FS; (c) Al P1; (d) Al P2; (e) Al R1; (f) Al R2; (g) Con P1; (h) Con P2; (i) Con P3; (j) Con R; (k) Aragonite.

Roughness of the surface material is seen to have an influence on the growth rate of coral across the surface in asexual reproduction (Figure 13). Substrates categorised with low surface roughness are seen to have a higher cross-sectional area of the coral new growth across the surface. Increase in degree of roughness reflects a decrease in surface area covered by the new growth of the coral. This general trend seems to be consistent throughout the duration of the experiment. As shown in SEM images and surface roughness measurements, the materials with higher roughness have higher surface area exposed due to the micro contours of peaks, valleys and voids. Therefore, a reason for the different growth rates between the roughness categories may be due to the nature of the growth of the coral, where in the process of growing across a surface it needs to

fill the space between the surface and the coral lappet. It may be that a substrate material with a higher surface area, greater valleys will require a larger volume to be filled before the new growth can extend further across the surface. The mechanisms of coral filling the voids between the new growth of the coral lappet and the substrate surface may show reduced linear extension growth, however it may correlate to an increase in the long-term strength of attachment of the coral fragment to the surface. This is currently an under studied area and further research is required to quantify and fully understand the mechanisms of coral growth that affect this [4]. Further work measuring attachment strength will enable this to be quantified.

Observations of marine fouling of the surface seems to show variation between the materials. Over the experiment period, the dominant fouling organism and the density of fouling visually differs between the materials and surface preparation techniques for the eleven materials in Figure 13. In general, materials classified to have a higher roughness were generally host to greater densities of marine fouling. This was observed even at early stages of the experiment at week three sampling and seen to increase in density from this time point.

The smoother surfaces such as the biopolymer and Al P1 seem to promote the growth of CCA. Surfaces with small, microscopic variations in surface topography including the alumina FS and the small porosity of Con P1 show a higher prevalence of brown algae species. It is noted that for AL P2, at the drilled porosity locations, algae growth is predominant at the circumference of these drill locations which is possibly correlated to the higher roughness which the drill bit generates when machining the surface. The total density of fouling seems to be higher for higher roughness materials. The surfaces of Al R1 and R2 still show the presence of CCA, however there is a shift in the predominant fouling organism to brown algae. The concrete surfaces seem to all show high density of fouling with mixed composition of types. The aragonite tile was one of the first tiles to foul quickly in the experiment, at nine weeks, it has a mixed cover of algae, although notably has a higher cover of green algae species than other tiles.

The increased surface area due to higher surface roughness and the added protection which the varying surface microtopography provides, is hypothesised to enable rapid establishment of fouling organisms. This may have some relationship to inhibiting asexual coral growth due to the competition between the fouling organisms and coral [5].

1.3 Main Conclusions and Recommendations

Overall, the material substrates seem to be viable for coral propagation. Results indicated that roughness has an influence on the coral growth rate across the surface area of the material. The material and chemical composition seem to have an influence on the growth of the corals. Further understanding is necessary to determine if the fouling community that the material supports or the material itself is the reason for variation in growth performance. From this study emerged a need to understand the impact of surface texture and chemical composition on marine fouling and how this could affect larval settlement and survival rate.

2 Impact of surface texture on fouling and larvae settlement

The main objective of this research work was to better understand and differentiate the impact of chemical composition and physical properties (surface porosity and texture) on marine fouling, larvae settlement, and survival rate.

2.1 Preparation of materials

The **concrete samples** were prepared following the standard AS 2350.12 – 2006 section 6 and 7. Adaptation of the standard mold size to a 90 x 90 x 10 mm PVC mold was made to achieve the desired dimensions to fit in the experimental tanks. The duration of time on the vibration table was modified to achieve variation in porosity. The tiles were leveled with a straight edge and placed in a controlled humidity and temperature chamber to cure. Chamber was set at a humidity of 90% and a temperature of 25°C. They were retained in the mold for 24 hrs before being removed and left in the controlled humidity and temperature climate for another 6 days at the same conditions. Table 4 shows the four different surface roughness profiles achieved through sand blasting at 100psi using various garnet grades: 80 Mesh, 40/60 Mesh, 30/60 Mesh, and 20/40 Mesh. 'CON-R2' was created with a smooth surface by evenly passing the sandblasting gun across the surface at 40 cm. A rougher surface was obtained by decreasing the distance of the sandblasting gun to 30 cm and prolonging the duration of each pass.

Fully sintered 95% pure alumina tiles (Al-R1) were sourced from Gongtao Ceramics, Shanghai, and used with no further surface modification. Partially sintered alumina tiles were sourced from Alpha Ceramics GmbH, Germany. Four different surface roughness profiles were achieved through sand blasting at 100psi with garnet grade, 80 Mesh, 40/60 Mesh, 30/60 Mesh and 20/40 Mesh (Table 4). A lower roughness surface named ‘Al-R2’ was achieved by evenly passing the sandblasting gun across the surface at approximately 40 cm from the surface. A higher level of roughness was achieved by decreasing the distance of the sandblasting gun to approximately 30 cm and increasing the duration of time taken for each pass of the sandblasting gun.

The **calcium carbonate** material was sourced from Oplusi. Four different surface roughness profiles were achieved through sand blasting at 100psi with garnet grade, 80 Mesh, 40/60 Mesh, 30/60 Mesh and 20/40 Mesh (Table 4). Horizontal sand blasting method was used to create the surface roughness profile.

Table 4: Material preparation and surface modification for concrete, alumina and calcium carbonate samples.

Material	Sand Grade	Concrete	Alumina	CaCO3
R1	---			
R2	80 Mesh	30-35 Sec	20-30 sec	15-20 sec
R3	40/60 Mesh	2-3 min	4-5 min	8-10 min
R4	30/60	4-5 min	7-8 min	15-16 min
R5	20/40	13-15 min	15-18 min	18-22 min

2.2 Characterization of materials

Surface morphology (roughness) of Alumina, calcium carbonate and concrete materials was characterized using laser scanning microscopy (LSM; LEXT OLS4100, Olympus Corporation, Japan Instrument). Five random areas of 2.583 x 2.574 mm were scanned of each material sample to obtain a 3D surface profile image.

The surface roughness of Alumina, calcium carbonate and concrete materials was measured using LSM. Determination of the mean roughness and maximum height of the roughness surface helps us to identify best suited surface roughness to coral growth. The maximum height (Sz) provides an understanding of the sum of the maximum peak and maximum pit height. The arithmetic mean (Sa) provides the average height of the sample profile for the area evaluated. A scale was created to evaluate the performance of surfaces with similar roughness by using the mean roughness data in Figure 14 to Figure 16. This scale (Table 6) allows for classification of materials into low, medium, and high roughness categories, which can be used to measure the impact of both material type and surface topography on coral growth. The summary of mean surface roughness categories and corresponding materials can be found in Table 6. As shown in Table 4, the alumina sample (A1-R1) without surface modification showed the smoothest with mean roughness value of 1.635 µm. However, sample Al-R2 to Al-R5, show high roughness with Sa value range between 13.064 to 15.463 µm. The maximum height (Sz) increases while increasing the surface roughness from Al-R1 to Al-R5. The three-dimensional profile Figure 14 shows that the Al-R5 has a high degree of waviness, with the surface being highly irregular in both the x and y planes.

The difference in 2D and 3D profiles between the five-calcium carbonate, which highlighting the variation in surface microtopography is presented in Figure 15. The rough surface exhibits high irregularity and waviness, while the smooth calcium carbonate surface has a more consistent profile with minimal variations in height. calcium carbonate surface roughness profiles are compared, and the results show distinct changes in the surfaces roughness depending on the method of sandblasting and garnet paper. The smooth calcium carbonate materials (CA-R1) showed mean height of 1.691 µm compared to the rough calcium carbonate materials (CA-R3) with mean height of 12.56 µm.

The changes on the surface roughness of concrete samples depending on the method of sandblasting and garnet paper. CON-Rl shows lower roughness with Sa and Sz value of 5.456 µm and 111 µm, respectively. CON-R5 is the roughest concrete material tested, which showed both the largest maximum height of 223 µm and mean arithmetic height of 16.018 µm. Comparison of the 2D and 3D profiles of the five concrete surfaces in Figure 16 clearly shows this variation in surface microtopography. The rough surface of the concrete had a high degree of irregularity and waviness, while the smooth surface had a more consistent and even profile with minimal variations in height.

Table 5: Surface roughness measurement of alumina, calcium carbonate and concrete.

Samples	Sq[µm]	Ssk	Sku	Sp[µm]	Sv[µm]	Sz[µm]	Sa[µm]
Al-R1	2.125	0.525	12.157	50.467	24.178	74.65	1.635
Al-R2	16.613	-0.416	3.481	75.351	73.479	148.83	13.064
Al-R3	18.611	0.234	3.003	78.577	70.63	149.208	14.808
Al-R4	17.359	-0.174	2.945	79.242	76.383	155.625	13.867
Al-R5	19.48	0.016	3.015	96.557	90.64	187.197	15.463
CA-R1	2.308	-0.203	20.012	38.863	51.479	90.343	1.691
CA -R2	9.838	-0.499	4.639	59.42	68.38	127.8	7.542
CA -R3	21.403	-2.274	15.424	68.933	148.403	217.336	12.048
CA -R4	13.29	-0.668	15.231	87.553	139.896	227.449	9.451
CA -R5	13.202	-0.846	28.176	94.345	126.725	221.07	7.557
CON-R1	7.142	0.541	5.882	62.891	49.005	111.897	5.456
CON -R2	12.574	0.12	3.646	71.64	53.966	125.606	9.92
CON -R3	15.415	-0.325	3.756	75.98	91.188	167.169	12.004
CON -R4	19.126	-0.814	6.36	77.157	117.933	195.09	14.574
CON -R5	20.785	-0.665	5.475	92.318	131.285	223.603	16.018

Al: Aluminium CA: Calcium Carbonate CON: Concrete

Table 6: Surface roughness Categories.

Roughness level	Mean surface roughness range	Samples
Low	0 – 4 µm	A1-R1
		CA-R1
Medium	4 – 8 µm	CA-R2
		CA-R5
		CON-R1
High	>8 µm	Al-R2
		Al-R3
		Al-R4
		Al-R5
		CA-R3
		CA-R4
		CON-R2
		CON-R3
		CON-R4
		CON-R5

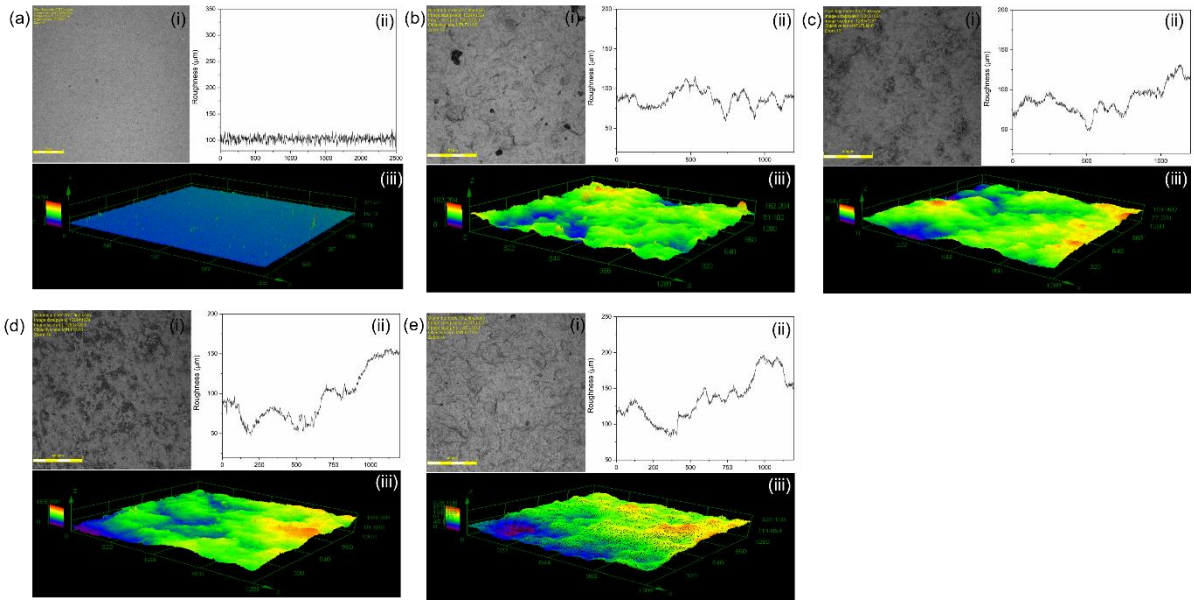

Figure 14: LSM (i) Surface Image, (ii) 2D Roughness Profile along x-axis, (iii) 3D Roughness Profile for: (a) Alumina-Roughness 1; (b) Alumina-Roughness 2; (c) Alumina-Roughness 3; (d) Alumina-Roughness 4; (e) Alumina-Roughness 5.

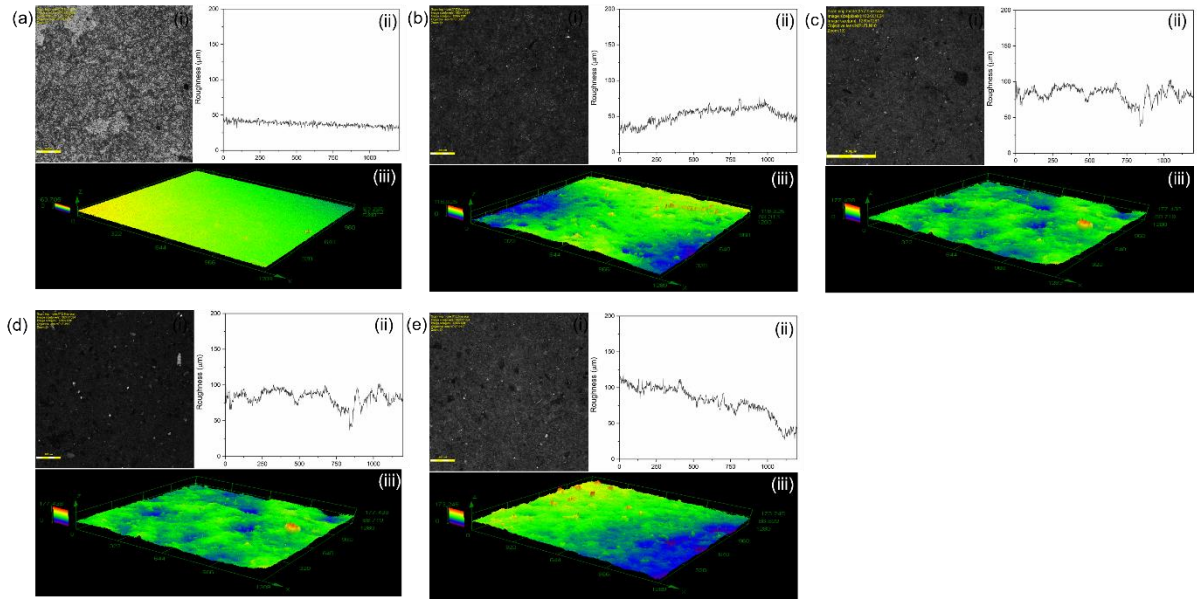

Figure 15: LSM (i) Surface Image, (ii) 2D Roughness Profile along x-axis, (iii) 3D Roughness Profile for: (a) Calcium Carbonate-Roughness 1; (b) Calcium Carbonate-Roughness 2; (c) Calcium Carbonate-Roughness 3; (d) Calcium Carbonate-Roughness 4; (e) Calcium Carbonate-Roughness 5.

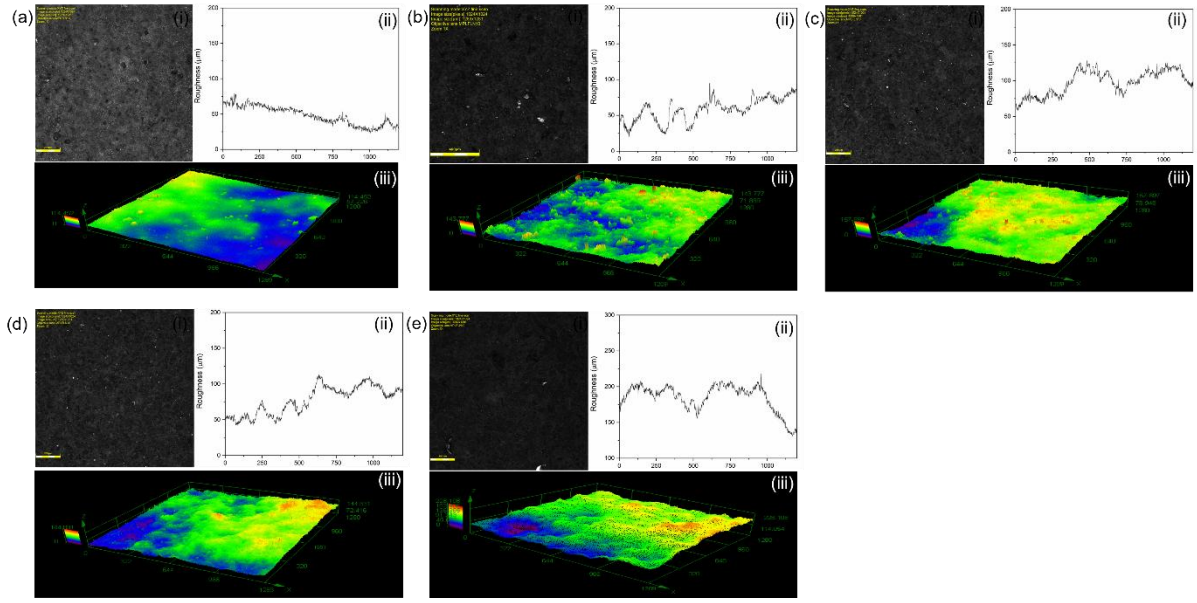

Figure 16: LSM (i) Surface Image, (ii) 2D Roughness Profile along x-axis, (iii) 3D Roughness Profile for: (a) Concrete-Roughness 1; (b) Concrete-Roughness 2; (c) Concrete-Roughness 3; (d) Concrete-Roughness 4; (e) Concrete-Roughness 5.

Surface morphology - SEM (Jeol JSM5410LV) was used to determine the microscopic surface morphology of representative samples of the settlement substrates. The samples were placed on carbon adhesive tape and coated with platinum to ensure the samples were electrically conductive and accurate results could be obtained. Three random locations were selected for each sample and imaged at three different magnifications of 5µm, 20µm, and 100µm. Coupled with Energy-dispersive X-ray spectroscopy (EDS), SEM-EDS enables the qualitative determination of the sample chemical composition.

SEM imaging was used to study the surface of the different materials, with a focus on understanding how coral attaches and grows on these surfaces. By combining the results from SEM with those from LSM measurements of surface roughness, the study was able to provide a more complete characterization of the types of surfaces that promote coral attachment. The images were taken at three different magnifications (500x, 2000x, and 10000x) to provide a comprehensive understanding of the surface topography and structure for the 15 different materials and tile surfaces tested.

SEM images in Figure 17 (a), (b), and (c) were used to compare the five alumina samples. Al-R1 had smooth surface as expected with even microstructure. However, Al-R5 shows an uneven and jagged microstructure, which was more irregular than that of Al-R1. This supports the results from LSM measurements of surface roughness. The modified surface of alumina samples had similar grain structure with a homogenous distribution of fine spherical grains. This is because they are all manufactured from the same base material. However, Al-R3, Al-R4, and Al-R5 had variations in surface topography compared to Al-R1. There was higher irregularity with larger scale peaks and valleys. As identified in the LSM analysis, the variation between surface modified alumina samples (Al-R2-Al-R5) is not significant, but Al-R5 had a higher degree of irregularity on the surface. Similarly, the samples of calcium carbonate material (Figure 18) displayed significant variation on their surface microtopography, characterized by a high number of large open pores and a high degree of irregularity. This is consistent with the results obtained from LSM measurements.

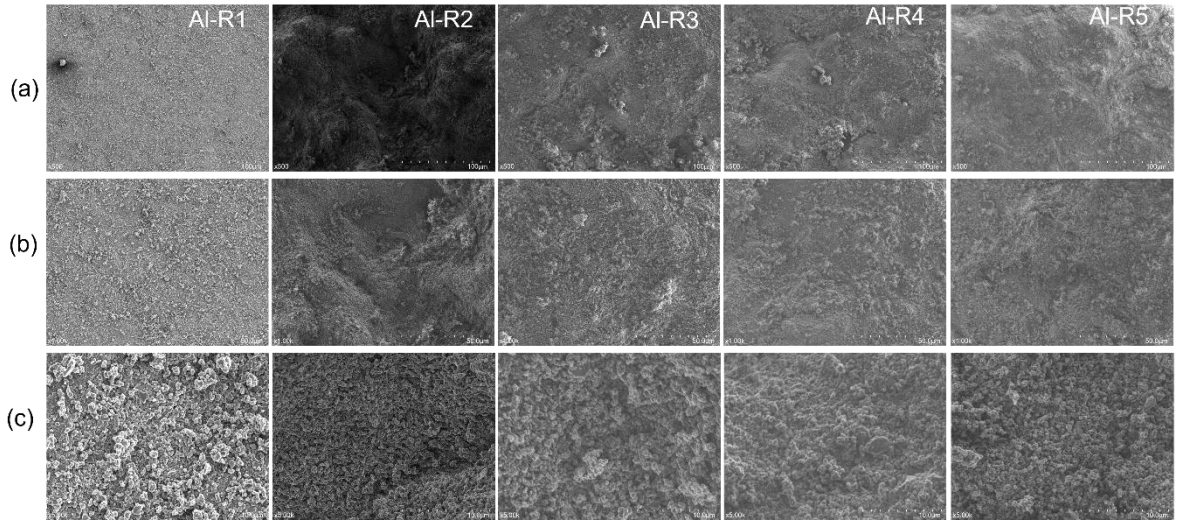

Figure 17: SEM images at (a) 100X, (b) 2000X and (c) 5000X scale of alumina samples.

The calcium carbonate samples (Figure 18) show high variation on the surface microtopography. The surface shows a high degree of large open pores. The surface is also highly irregular which supports the results obtained through LSM. The concrete surfaces have distinct variations in topography and grain size. CON-Rl has smooth surface with smaller grains, while CON-R3, CON-R4, and CON-R5 have rough and irregular surface. Figure 19 illustrates these differences, with sample CON-R1 having an even microstructure compared to the rough samples (CON-R2 to CON-R5).

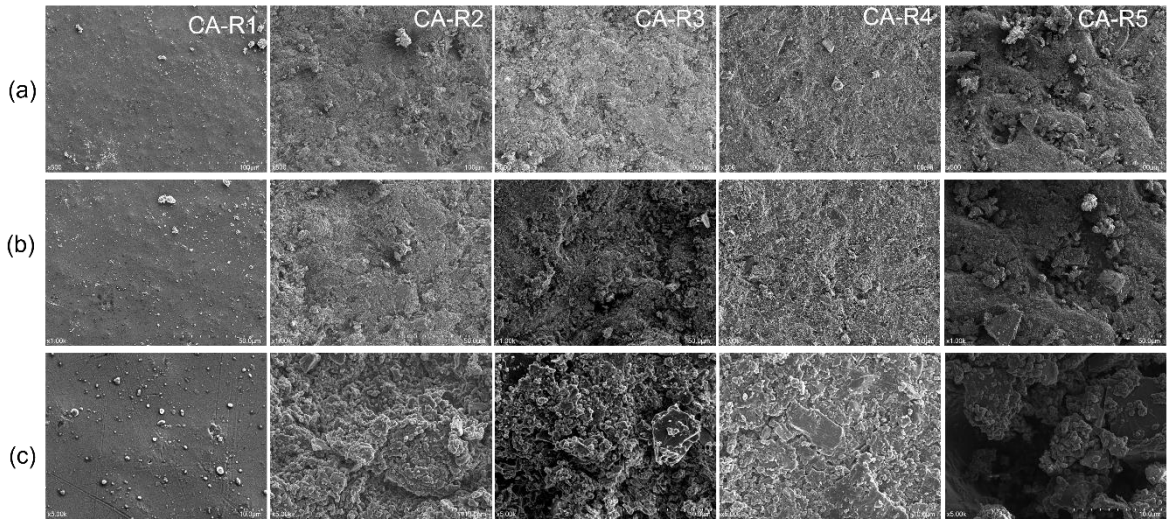

Figure 18: SEM images at (a) 100X, (b) 2000X and (c) 5000X scale of calcium carbonate samples.

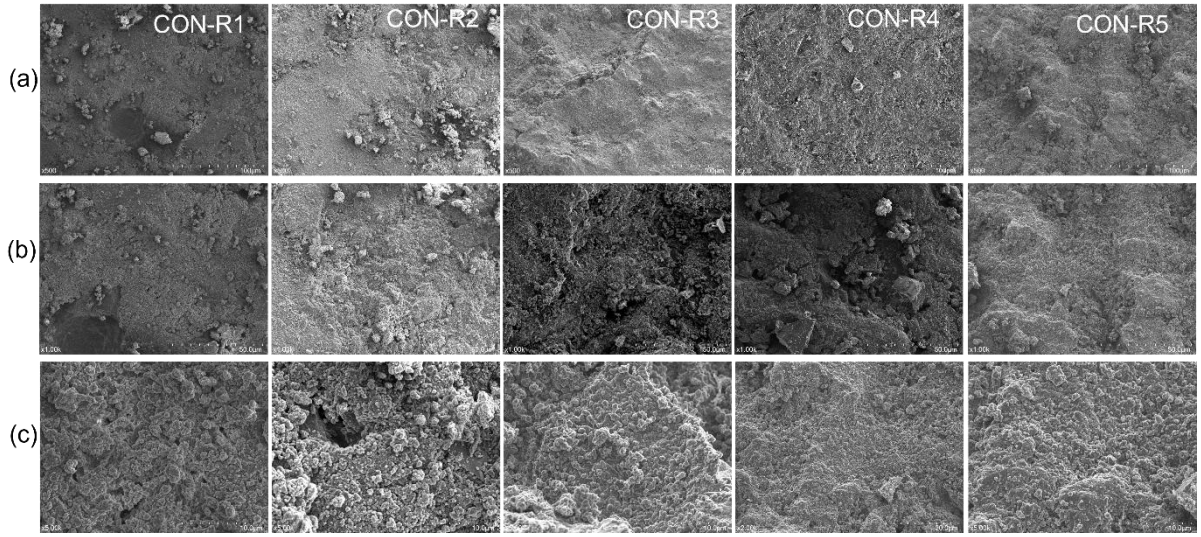

Figure 19: SEM images at (a) 100X, (b) 2000X and (c) 5000X scale of concrete samples.

SEM-EDS was used to analyze the chemical composition of the materials. By identifying the composition at the surface, we were able to determine the importance of the chemical composition of the substrate versus the physical surface topography of the material. The alumina material had a high presence of oxygen between 47-45 wt.%, in all samples. The samples were found to be highly pure, with 52.9 wt.% aluminum present (in average). Small amounts of impurities in the form of silicon were present in the surface-modified partially alumina samples. Additionally, trace amounts of calcium were found in samples Al-R4 and Al-R5, at 0.3 wt.% and 0.6 wt.%, respectively. These values are low and may be due to sample contamination during sand blasting.

The concrete samples were found to contain calcium, magnesium, aluminum, silicon, and oxygen, as shown in Figure 20 (a). Calcium was found to be the most prevalent element in all five material surfaces, with the highest concentration of 48.2 wt.% in CON-R1. The other samples, CON-R2, CON-R3, CON-R4, and CON-R5, had calcium concentrations of 47.37, 30.66, 33.86, and 36.79 wt.%, respectively. Aluminum was also present in the concrete samples, with concentrations ranging from 6.12 to 13.7 wt.% for all samples, indicating a similar chemical makeup. Silicon was also found to be present in higher concentrations in three concrete samples (CON-R3, CON-R4 and CON-R5), with the highest concentration of 10.79 wt.% found in CON-R5. The analysis of the chemical composition of these samples shows that the concrete samples have a very similar chemical makeup across their surfaces. Trace metals, including potassium, iron, and sulfur, were also found in the three materials.

The calcium carbonate samples mainly composed of calcium and oxygen. As shown in Figure 20 (b), CA-R1 have the highest content of calcium (66.02 wt.%). After surface modifications the amount of calcium decreased, and the lowest value was for CA-R5 (34.74 wt.%). The EDS is just a qualitative analysis of the chemical composition and provides an overview of the elements present but does not provide accurate results of the chemical composition.

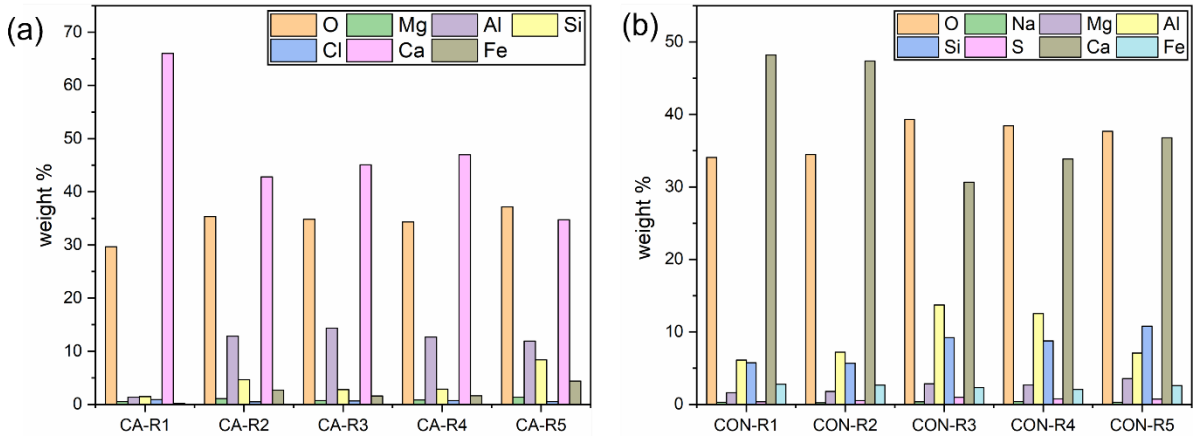

Figure 20: Chemical composition of material by weight percent: (a) calcium carbonate materials and (b) concrete materials.

2.3 Experimental Design

A mesocosm experiment (10 weeks) was carried out in the indoor aquaria at the National Sea Simulator (SeaSim) of the Australian Institute of Marine Science (AIMS) in Townsville, Australia. Prior to the experiment, the tiles were conditioned for 6 weeks. *Acropora tenuis* was used for this experiment, which was collected from the reefs around the Palm Island Group, Australia (18° 45′ 56.4″ S 146° 32′ 2.58″ E) in October 2022.

2.4 Main Conclusions and Recommendations

The results from this work showed that in general the surface roughness of the substrate materials had minimal impact on algae community and coral recruitment. The outcomes from this work might be impacted by the strong effect of the tanks' algal community. In general, coral larvae preferred to settle on concrete tiles than on alumina or calcium carbonate tiles potentially because of the high CCA presence on the concrete tiles. Further, the survivorship of coral spat declined significantly over the course of 10 weeks across all treatments; however, the spat survival rate was higher for the calcium carbonate (73.5%) compared with alumina (37.8%) and concrete (39%).

3 3D Printing of Ceramic Substrates for Coral Larvae Settlement

The main objective of this study was to understand the impact of porosity on sexually reproduced larvae settlement rates. A two-month experiment was performed to capture two out-of-season spawning events across three species of coral, completed at both a 10 mL and 15 L scale at the Australian Institute of Marine Science (AIMS) SeaSimulator research laboratory. The three sexually reproduced species that were tested include *Montipora aequituberculata* (Maeq), *Mycedium elephantotus* (Mele), and *Acropora loripes* (Alor). Two ceramic materials, Alumina and Hydroxyapatite, were used to form the basis of comparison, with pore sizes ranging from 0 µm to 900 µm examined to determine the preferred porosity. The settlement rates of the coral were compared based on their success against the varying treatment, material and porosity configurations, with inter- and intra-species relationships observed.

3.1 Materials Preparation

The designs were each created using the software package nTopology with pore sizes intended to range between 0 µm and 1000 µm. A total volume of 2 x 2 x 8 mm was selected to act as an extension to previous studies conducted by AIMS, with a dense tab with no pores initially selected to act as a base control to determine whether the larvae showed preferential signs to specific porosity, or just the material itself. Five increments were chosen through collaboration with AIMS, with these initially established to be 0 µm, 400 µm, 600 µm, 800 µm, and 1000 µm; 400 µm was selected to be the smallest pore size as this was the smallest size that could be manufactured and post-processed effectively. When modelling these designs, it was also found that the ratio of pores to flat surface had to be maintained across all pore sizes to ensure that the larvae was settling on a specific pore size because that is what it prefers, rather than it simply being more abundant; this ratio was maintained between 0.779 and 0.8684. This value was not able to be completely consistent amongst pore sizes due to the parameters of the design requirements; pores had to be whole and could not be cut off by the 2 x 8 mm top surface restriction. As a result, 1000 µm could not be used and this increment was lowered to 900 µm. Figure 21 shows the different geometries/pore size tested.

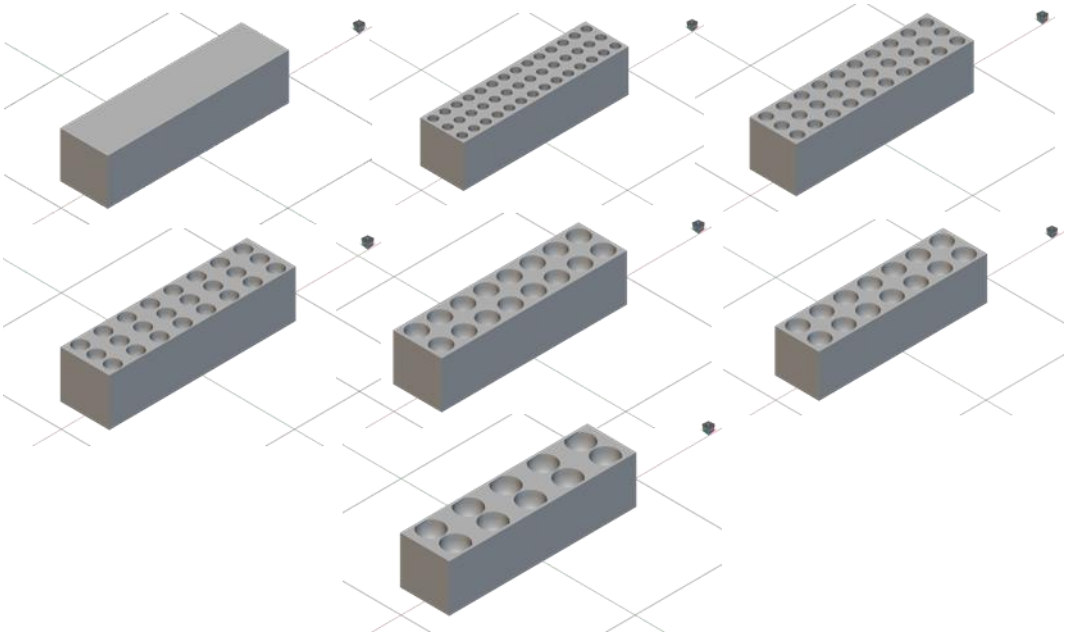

Figure 21: The seven tabs design produced for the coral larvae settlement experiment, pore size varies between 0 and 900 µm.

The Alumina tabs were manufactured using Al:E03 slurry sourced from 3DCeram, whilst the Hydroxyapatite tabs were manufactured using HAP-E01 slurry also sourced from 3DCeram. The Alumina slurry is capable of obtaining the following microstructure properties: density of >3.9 g/cm^3 and a grain size after sintering of 2.2 µm. Its mechanical properties include a 4-pt bending strength of 397 MPa, a Vickers hardness of 16.4 GPa, and a fracture toughness of 4 MPa.m$^{0.5}$. Similarly, the HAP slurry has the following microstructure properties: densification rate of >96%, density of >1.5 g/cm^3, and a grain size after sintering of 2 µm. The mechanical properties include a 4-pt bending strength of 107 MPa with general properties such as a crystallinity of >95% listed in addition. All tabs were printed from 3D Ceram CERAMAKER 100 printer (C100) which is a Class 1 Laser 3D printer machine, where they were then debound and sintered using either a Labec Horizontal Tube Furnace or MTI Corporation Bench-Top Muffle Furnace; both of these furnaces are capable of operating at maximum temperatures of approximately 1700°C.

1000 tabs were required to be manufactured for the May spawning, with 100 tabs of each geometry needing to be produced, half of which will be conditioned for between 11-13 days. 120 tabs were produced for each geometry to accommodate for any damage caused during post-processing resulting in a total of 1200 total tabs produced for this spawning.

The manufacturing process for the June spawning was the same as that for the May spawning, however, the pattern of attachment onto the concrete tiles was different; this resulted in 800 tabs produced being used across two repeats. 400 tabs were conditioned for 28 days, whilst 400 remained unconditioned; Figure 22 illustrates the hierarchy of settlement substrates with remaining tabs used in well plates. Additionally, four tiles were left blank with two conditioned acting as a positive control, and two unconditioned to act as a negative control and ensure the tabs were effective in promoting settlement.

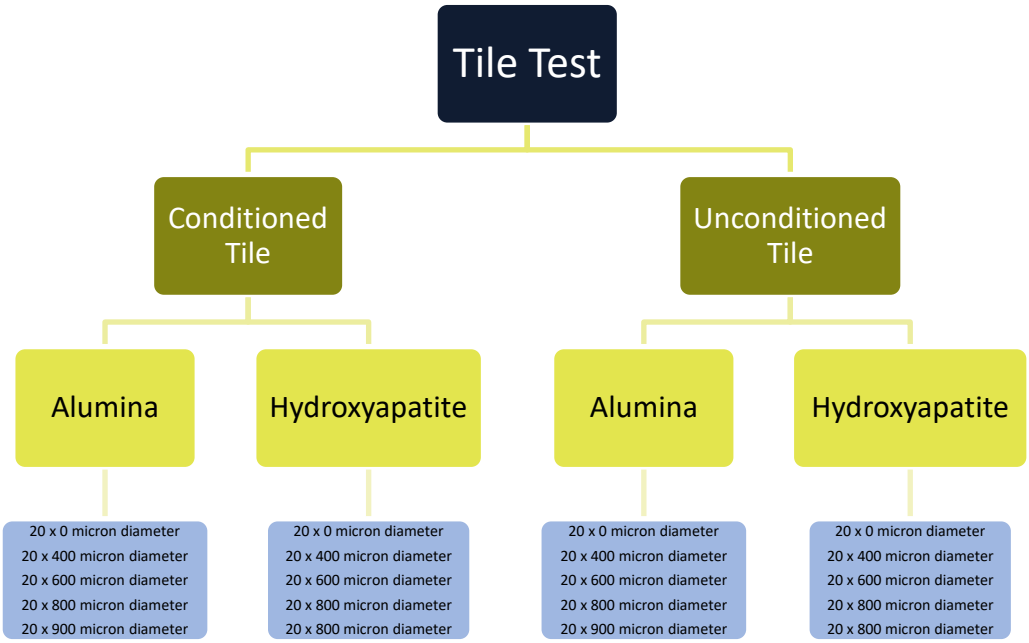

Figure 22: *Settlement substrate hierarchy for June spawning.*

The ceramic tabs were glued onto concrete tiles. These tiles were fabricated at JCU concrete laboratory using "chocoblock" molds and a concrete mix composed of cement, sand, fly ash, and water. For one tile, the mixture was composed of 480 g of general-purpose cement, 400 g of sieved sand (500 µm), 120 g of fly ask, and 180 mL of water; these values were multiplied to make five tiles at a time using a CreteAngle Forced Action Pan Mixer. The cement and fly ash were first mixed using water for 30 seconds at a slow speed, where the fine CEN standard sand was then added and mixed for another 30 seconds at a fast speed. The mixture was then left for 90 seconds to form cementation and mixed again for another 60 seconds at a fast speed to ensure a homogeneous, workable consistency. The chocoblock molds were sprayed with canola oil to act as

a lubricant and assist in the de-molding process, and the mixture was poured in and spread with a scraper. The tiles were left to dry for seven days to achieve maximum strength.

A grid pattern was drawn on the flat side of the concrete tile to create a template for the checkerboard pattern that the tiles were to be glued on for the May spawning; this grid followed that of the chocoblock molding. From here, randomized mud maps for five repeats per conditioning were created to ensure data was able to be categorized correctly after spawning. Excel functions were used to generate a randomized list of the available geometrical combinations with an example shown in Figure 23.

HAP 900 T1		AI 400 T10		AI 0 T10		HAP 400 T8		AI 0 T6	
	HAP 800 T6		AI 600 T4		HAP 800 T3		HAP 900 T8		HAP 0 T4
HAP 800 T8		AI 900 T8		AI 0 T7		HAP 900 T6		HAP 400 T9	
	HAP 400 T4		AI 400 T8		HAP 800 T2		AI 800 T6		HAP 400 T2
AI 0 T3		AI 800 T4		HAP 0 T10		AI 900 T2		HAP 400 T1	
	HAP 600 T8		HAP 900 T4		AI 0 T4		AI 400 T5		AI 800 T1
AI 600 T8		AI 600 T10		HAP 400 T7		HAP 0 T5		AI 900 T4	
	AI 600 T6		HAP 900 T3		AI 400 T9		HAP 0 T3		HAP 600 T1
HAP 0 T2		AI 0 T1		AI 900 T10		HAP 600 T2		HAP 400 T6	
	AI 900 T5		AI 0 T5		AI 900 T1		AI 900 T6		HAP 600 T7
HAP 600 T5		HAP 400 T5		HAP 600 T10		AI 600 T3		HAP 900 T5	
	HAP 600 T9		AI 900 T3		HAP 900 T10		AI 600 T5		HAP 800 T4
HAP 600 T3		AI 400 T6		AI 900 T9		AI 400 T2		AI 0 T2	
	HAP 900 T9		HAP 800 T5		HAP 600 T4		HAP 0 T7		HAP 800 T9
AI 900 T7		HAP 400 T3		HAP 600 T6		AI 0 T9		HAP 0 T1	
	HAP 800 T7		AI 400 T3		AI 400 T7		HAP 0 T8		HAP 800 T10
HAP 900 T2		HAP 0 T9		HAP 400 T10		AI 600 T7		AI 800 T10	
	AI 800 T8		AI 400 T4		AI 400 T1		AI 600 T2		AI 800 T3
AI 800 T7		AI 800 T9		HAP 800 T1		AI 800 T5		AI 800 T2	
	HAP 900 T7		AI 0 T8		HAP 0 T6		AI 600 T1		AI 600 T9

Figure 23: *Mud map of Tile 1 Conditioned (Treated) for May spawning.*

Figure 24 shows the grid pattern drawn onto the tiles with the tabs glued on using Gorilla Super Glue Gel. Once glued, the tiles were left to dry for another 24 hours and then placed in a tub of water with continuous lightly flowing freshwater for 72 hours to rinse any unwanted residual chemicals or concrete dust from the surface of the tiles.

Figure 24: *Tiles prior to coral larvae settlement in May spawning.*

The June spawning differed slightly as the methodology was revised to improve on limitations observed during the May spawning. The pattern of tabs was altered to be glued onto every grid unit rather than in a checkerboard pattern resulting in only two repeats being feasible with the number of tabs originally produced. An example image of the mud maps created, and practical implementation of tile gluing is shown below in Figure 25 and Figure 26, respectively. These tiles for the June spawning underwent the same post-fabrication cleaning processes that were performed for the May spawning tiles.

Al 800 T3	HAP 900 T1	HAP 0 T7	HAP 600 T2	Al 400 T9	HAP 400 T8	HAP 900 T3	HAP 900 T5	Al 800 T5	Al 600 T9
Al 800 T1	HAP 600 T7	Al 400 T8	HAP 800 T1	HAP 400 T6	HAP 400 T7	HAP 600 T8	Al 0 T3	HAP 800 T4	HAP 0 T4
HAP 900 T7	HAP 900 T10	Al 900 T4	Al 0 T5	Al 800 T8	Al 900 T7	Al 800 T10	HAP 600 T3	HAP 800 T6	HAP 900 T9
Al 900 T9	HAP 400 T5	HAP 400 T7	Al 800 T4	Al 800 T9	HAP 800 T10	Al 0 T10	Al 800 T1	Al 800 T2	Al 900 T5
HAP 900 T5	HAP 900 T4	Al 900 T6	Al 400 T6	HAP 800 T9	HAP 600 T2	Al 0 T9	Al 900 T8	HAP 600 T6	Al 800 T4
HAP 400 T2	HAP 800 T8	Al 400 T2	HAP 800 T4	HAP 0 T6	HAP 900 T1	Al 0 T7	Al 600 T7	HAP 600 T4	Al 400 T5
Al 900 T5	HAP 900 T8	Al 600 T6	HAP 600 T9	Al 400 T10	Al 900 T6	HAP 0 T9	Al 900 T2	Al 0 T8	HAP 0 T10
Al 900 T8	Al 800 T5	HAP 0 T1	Al 800 T7	HAP 600 T8	Al 900 T1	HAP 600 T10	Al 0 T6	Al 400 T9	HAP 800 T2
HAP 900 T6	HAP 400 T4	Al 900 T3	Al 600 T3	HAP 400 T8	HAP 400 T1	Al 900 T4	Al 0 T5	HAP 800 T7	Al 900 T10
Al 900 T10	HAP 900 T9	Al 0 T6	Al 0 T1	HAP 400 T9	Al 600 T8	Al 400 T7	Al 600 T6	HAP 400 T10	HAP 800 T1
Al 0 T9	HAP 600 T1	HAP 800 T7	HAP 900 T2	Al 400 T3	Al 800 T9	HAP 0 T3	HAP 600 T5	HAP 400 T5	HAP 900 T6
Al 600 T1	HAP 800 T3	HAP 800 T6	Al 800 T10	HAP 0 T4	HAP 800 T9	HAP 0 T2	Al 600 T4	HAP 900 T4	Al 800 T3
Al 800 T2	HAP 400 T1	HAP 0 T3	Al 600 T2	Al 400 T4	Al 900 T9	Al 800 T6	Al 800 T8	Al 0 T4	Al 0 T1
Al 0 T2	HAP 400 T3	HAP 0 T8	Al 600 T10	Al 400 T7	Al 900 T3	Al 400 T10	Al 600 T2	Al 800 T7	HAP 400 T3
Al 900 T7	Al 600 T9	Al 0 T8	HAP 600 T4	HAP 400 T10	HAP 600 T1	HAP 600 T7	Al 0 T2	HAP 0 T5	HAP 0 T1
Al 0 T4	Al 400 T1	Al 0 T7	HAP 600 T10	HAP 800 T5	HAP 900 T8	Al 400 T1	HAP 900 T2	HAP 800 T3	HAP 400 T9
Al 0 T3	Al 600 T5	Al 400 T5	Al 900 T1	HAP 600 T3	Al 400 T8	Al 400 T3	HAP 800 T8	Al 600 T1	Al 400 T2
HAP 0 T5	Al 600 T7	HAP 600 T6	HAP 800 T2	Al 600 T4	HAP 400 T4	Al 600 T5	HAP 600 T9	HAP 0 T6	HAP 900 T7
HAP 0 T10	HAP 800 T10	Al 0 T10	Al 600 T8	HAP 600 T5	Al 400 T6	HAP 800 T5	HAP 400 T6	HAP 900 T10	Al 400 T4
Al 800 T6	HAP 0 T2	Al 900 T2	HAP 900 T3	HAP 0 T9	HAP 400 T2	HAP 0 T7	Al 600 T3	HAP 0 T8	Al 600 T10

Figure 25: Mud map of Tile 1 Conditioned (Treated) for June spawning.

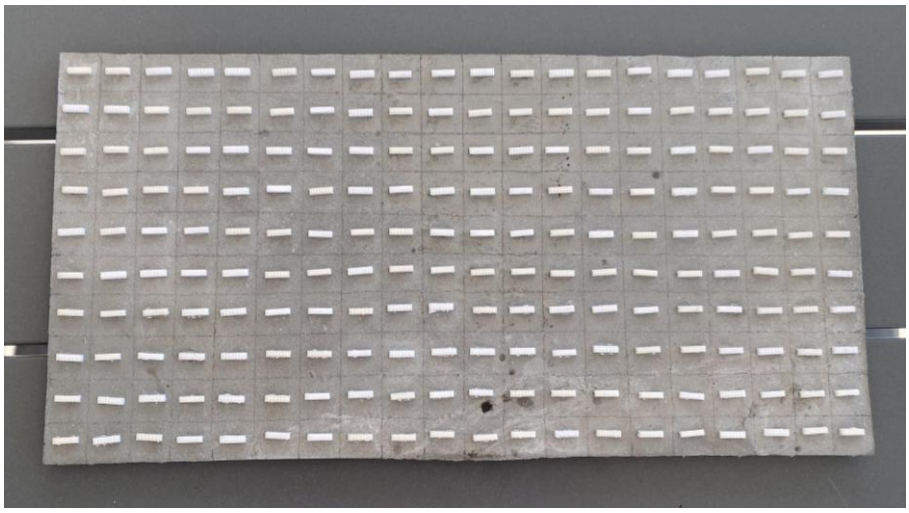

Figure 26: Tiles prior to coral larvae settlement in June spawning.

3.2 Materials Characterization

SEM enabled the identification of grain size and porosity of both materials tested against coral larvae settlement. Preferential selection patterns were able to be analysed with respect to the surface properties of Alumina and HAP potentially providing justification for any trends observed. Figure 27 and Figure 28 display the SEM images obtained for both Alumina and HAP, respectively. SEM images were taken at five different magnifications: 500x, 1000x, 2000x, 5000x, and 10000x, with these variances allowing the images to thus be seen with five different scale bars: 100 µm, 50 µm, 20 µm, 10 µm, and 5 µm, respectively.

(a) 100 µm, 500x Mag. (b) 50 µm, 1000x Mag. (c) 20 µm, 2000x Mag.

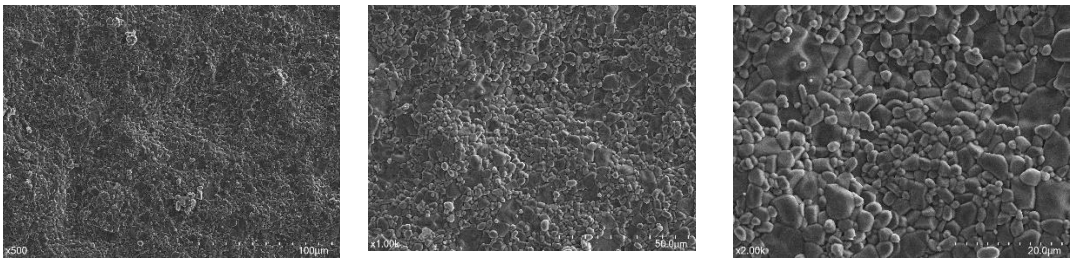

(d) 10 µm, 5000x Mag. (e) 5 µm, 10000x Mag.

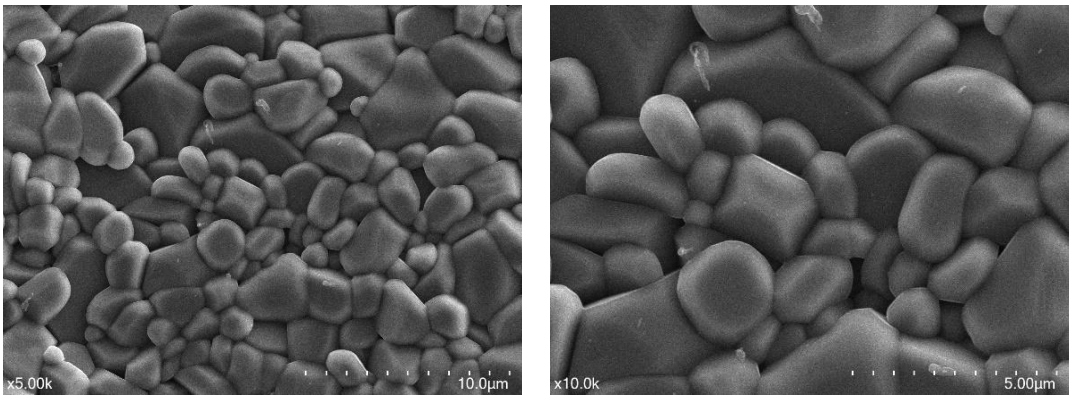

Figure 27: SEM images for Alumina after sintering.

(a) 100 µm, 500x Mag. (b) 50 µm, 1000x Mag. (c) 20 µm, 2000x Mag.

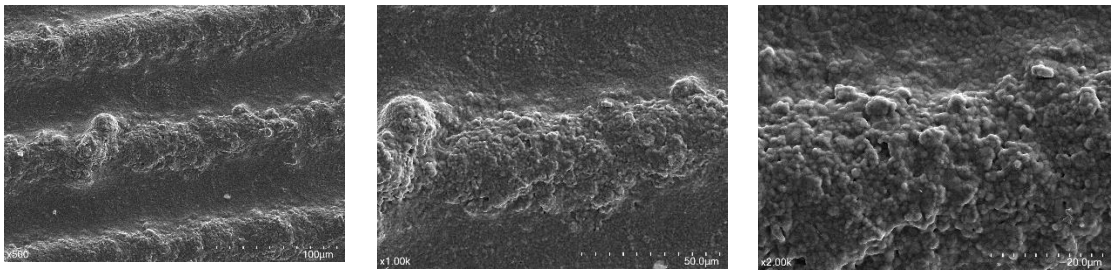

(d) 10 µm, 5000x Mag. (e) 5 µm, 10000x Mag.

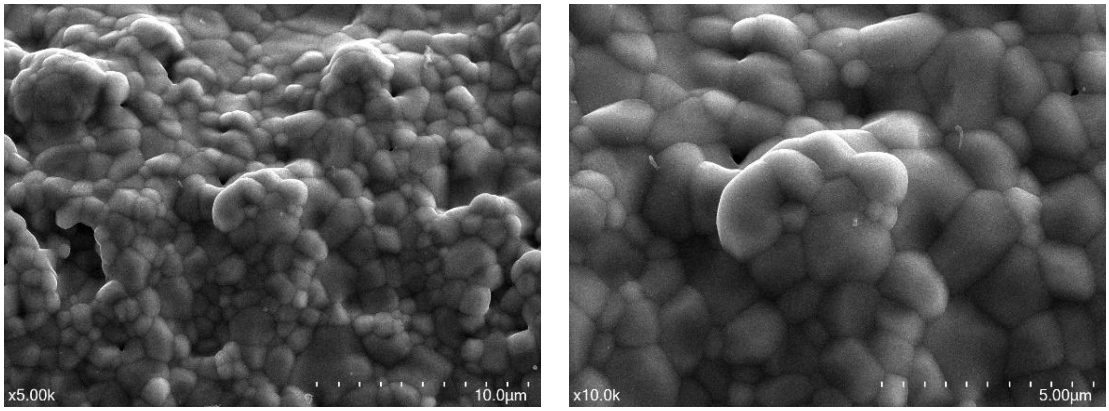

Figure 28: SEM images for HAP after sintering.

The Alumina material tested, shown in Figure 27, revealed a relatively homogenous distribution of rounded grains. Using ImageJ software, ten grain measurements were taken to find an average length of 2.22 µm. The surface morphology of the grains is smooth in texture, whilst each visible grain has distinct borders separating them from surrounding grains with minimal angular edges or large open pores. Comparatively, the HAP shown in Figure 28 indicates diffuse grains as there are fewer distinct borders with the grains appearing to morph to each other in clusters. The grains seen are rounded, similar to that of Alumina, however, slightly smaller, measured to have an average length of 1.99 µm. Finally, when using a 100 µm scale at 500x magnification, the Alumina and HAP appear to be very different. The Alumina in Figure 27 (a) is very homogeneous, and whilst the individual grains can be seen, large variations in the surface patterns cannot be identified. Alternatively, deep troughs are seen for HAP in Figure 28 (a), indicative of either greater areas of surface porosity that formed during the processing of the material, or decomposition of certain phases during sintering.

X-Ray diffraction (XRD) was used to identify and quantify the crystalline structures present in both alumina and hydroxyapatite. The XRD results prove that the alumina tabs were composed of alpha alumina while the XRD of the hydroxyapatite tabs confirm that the material was mainly hydroxyapatite and no other crystalline structures were present.

3.3 Larvae Collection and Settlement Experiment

For the May event, *Maeq* and *Mele* larvae spawned on Thursday May 23rd, 2024, with each collected into two 70 L tanks and filled with approximately 100,000 larvae. Larvae was collected from these large tanks by submerging a sieve into the water and moving it around the tank for approximately 30-seconds. The sieve was then quickly transferred into a full 3 L beaker of water and the larvae was washed out of the sieve using freshwater. This process was repeated numerous times depending on the number of larvae needing the be collected; for the tests involving well plates, including the competency and blank pre-tests, fewer passes were required as only 10 larvae were needed per well, whereas the tile experiments required approximately 7 passes being that 5000 larvae were needed.

For the June event, Alor larvae spawned on Tuesday June 25th, 2024, after the full moon on Friday June 21st, 2024, again collected into a 70 L tanks and filled with approximately 100,000 larvae. Larvae was collected from this tank in the same manner as the May spawning for both the well plate and tank experiments.

For the primary tile experiments, one tile was placed per tank in a random distribution as shown in Figure 29. The larvae were again collected on Monday May 27th, 2024, at four days old. As a 3 L beaker was used to collect the larvae, 300 mL of water was collected and placed per tank to ensure an average of 500 larvae were present in each tank.

Unconditioned Tile 2	Conditioned Tile 5	Conditioned Tile 3	Conditioned Tile 2	Conditioned Tile 1
Unconditioned Tile 3	Conditioned Tile 4	Unconditioned Tile 1	Unconditioned Tile 5	Unconditioned Tile 4

Figure 29: Maeq tile distribution across ten tanks.

For the primary tile experiments conducted after the June spawning, one tile was again placed per tank in a random distribution as shown in Figure 30. The larvae were collected on Sunday June 30th, 2024, at five days

old. As a 3 L beaker was used to collect the larvae, 300 mL of water was collected and placed per tank to ensure an average of 500 larvae were present in each tank.

Conditioned Tile 2	Unconditioned Blank Tile 1	Conditioned Tile 1	Unconditioned Blank Tile 2
Unconditioned Tile 1	Unconditioned Tile 2	Live Blank Tile 1	Live Blank Tile 2

Figure 30: Alor tile distribution across eight tanks.

3.4 Main Conclusions and Recommendations

Regarding the effect of CCA conditioning, the results presented were unanimous; conditioned tabs were far more effective in promoting settlement compared to unconditioned tabs. For the first experiment conducted on Maeq larvae within well plates, conditioned Alumina exceeded the success of unconditioned Alumina increasing in percentage by 74.53% (6.63% to 81.16%), and conditioned HAP to unconditioned HAP by 39.86% (33.24% to 73.10%). These trends were replicated for Mele, albeit at a much lower magnitude, where unconditioned tabs were seen to have 0% settlement compared to conditioned Alumina and HAP recorded to be 1.44% and 5.26%, respectively. Finally, at the same scale but during the June spawning, Alor results were found to increase by 110% from 17.32% to 36.46% for Alumina when comparing unconditioned to conditioned, and 159% for HAP unconditioned to conditioned from 14.89% to 38.59%. At a larger scale, the trends were again reproduced with Maeq having only 12 coral spats settle on unconditioned tabs, compared to 25 settling on conditioned tabs indicating another increase greater than two times that of unconditioned, with similar results obtained for Alor larvae with 0 settlement experienced across all unconditioned tabs, compared to 310 coral spats settled on conditioned tabs. The vast differences in magnitude were attributed to varying CCA coverage, larvae health, and available tabs.

In conclusion, a clear preference for settlement has been identified and is conducive across all three species tested. Conditioned tabs were drastically better than unconditioned with HAP presenting better results than Alumina. The most effective pore size was almost unanimous at 800 µm, irrespective of larvae species and their individual diameters. Some of the trends observed were found to align with previous literature, some findings were new, and some were found to disagree with past research, thus, the final recommendation based on experimental findings was to use conditioned HAP tabs with a fabricated porosity of 800 µm to obtain the highest settlement percentage. Despite these findings, the process of producing the tabs also must be considered regarding the ease of fabrication and related expenses. The Alumina was much easier to handle during fabrication than HAP, resulting in fewer breakages and thus less wastage, decreasing overall cost of production. Raw costs of the Alumina slurry are also significantly lower than that of HAP resulting in a compromise needing to be determined.

4 Future Work

The ability to manufacture or control the surface roughness of a given surface designed for the attraction and retention of coral larvae in a controlled repeatable manner may provide another option for coral attraction. Previous studies conducted with the use of alumina, concrete and calcium carbonate with a focus on the surface roughness (S_a and S_z) indicated that the inclusion or presence of surface roughness may attribute to a preferable surface finish to assist with coral settlement and survivorship over the long time.

With the manufacturing and design capabilities currently available via implicit modelling and design, methods exist to mimic roughness surface profiles from laser scanned data to be incorporated into the 3D printed structure (Figure 31). This ability to replicate the roughness profile can also be tailored to obtain specific arithmetic mean and maximum heights to suit the specific requirements of the varying species of coral larvae. Further, the laser scanned technique should be used to scan and obtain geometries natural available that have high coral settlement and survival rates.

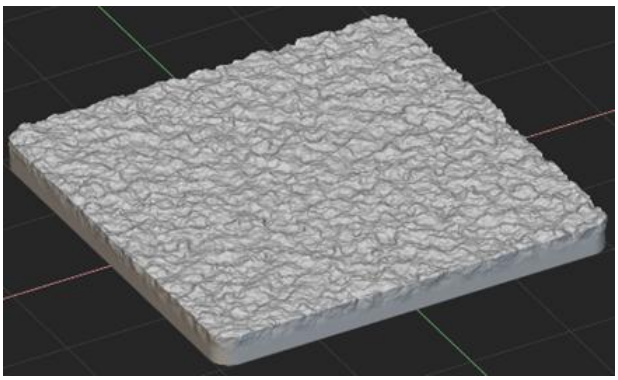

Figure 31: Rough surface model to be 3D printed.

The research conducted into developing coral larvae substrates housing dimensional pores indicated that 800 µm pores were suited for retention of coral larvae. Based on this work, further research can be conducted into the use of TPMS structures as a method of tailoring these highly porous lattice structures for the benefit of a suitable housing for coral larvae. Typical of both gyroid and diamond TPMS structures although not restricted to these two lattice types; unit cell size, wall thickness, and mid-surface offset parameters all result in creating a lattice structure whereby resulting pore sizes for the given lattice structure can be obtained. By designing these TPMS structures around the desired pore sizes the potential exists for developing 3d printed TPMS structures (Figure 32) not obtainable via other methods of manufacture at the small geometrical scale required for larvae housing.

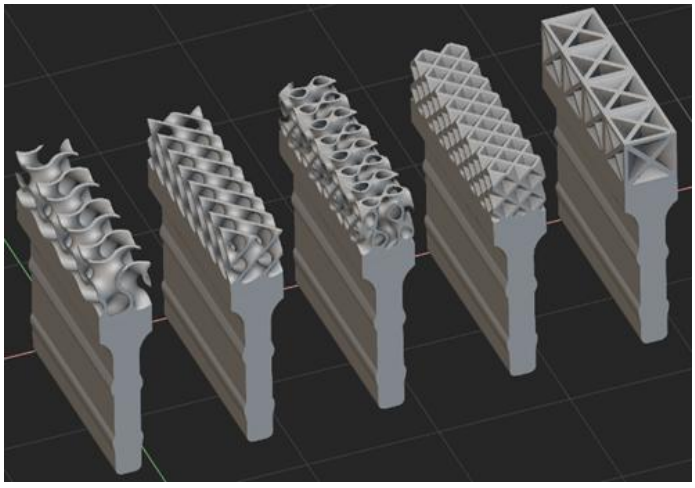

Figure 32: Examples of TPMS structures to be considered in the near future.

In the previous experiments the small tabs were glued onto the surface of the chocoblocks, however, an assembling process must be developed to insert the TPMS structures into the concrete tiles. The tabs have a huge potential in terms of scaling up the coral cultivation as they require small volume to be conditioned. Further, the geometry of the tabs can be tailored to different coral species in order o improve the settlement rate. The geometry of the tabs could be similar to filters and house some chemicals to induce coral larvae settlement.

References

[1] *AS 2350.12 Methods of testing portland, blended and masonry cements, Method 12: Preparation of a standard mortar and moulding of specimens*, 2006.

[2] *ISO 25178-2 Geometrical product specifications (GPS) — Surface texture: Areal — Part 2: Terms, definitions and surface texture parameters*, 2012.

[3] *ISO 18754:2020 Fine ceramics (advanced ceramics, advanced technical ceramics) — Determination of density and apparent porosity*, 2020.

[4] B. Lewis, "Clast assimilation and substrate attachment in Acropora millipora," School of Earth, Environmental & Biological Sciences Past QUT, 2019.

[5] J. Tebben, J. R. Guest, T. M. Sin, P. D. Steinberg, and T. Harder, "Corals Like It Waxed: Paraffin-Based Antifouling Technology Enhances Coral Spat Survival," *PLOS ONE,* vol. 9, no. 1, p. e87545, 2014, doi: 10.1371/journal.pone.0087545.

REEF RESTORATION & ADAPTATION PROGRAM

Australian Government | Reef Trust

Great Barrier Reef Foundation

Australian Government | Australian Institute of Marine Science | CSIRO | James Cook University Australia | QUT | Southern Cross University | The University Of Queensland Australia